Supplementary Information for

Nature of a Long Carbon–Carbon Bond Beyond 2.0 Å

Takashi Kubo, Yuki Suga, Daisuke Hashizume, Hiroki Suzuki, Tatsuya Miyamoto, Hiroshi Okamoto, Ryohei Kishi, and Masayoshi Nakano

Correspondence to: kubo@chem.sci.osaka-u.ac.jp (T.K.); hashi@riken.jp (D.H.)

Table of Contents

Materials and Methods

Materials

General: All experiments with air- or moisture-sensitive compounds were performed in anhydrous solvents under nitrogen atmosphere in well-dried glassware. 1,3-dimethyl-2-imidazolidinone (DMI) and tetrahydrofuran (THF) were purchased from KANTO Chemical Co., Inc., Japan as anhydrous solvents. Hexane was dried and distilled over calcium hydride under argon atmosphere. Column chromatography was performed with silica gel [Silica gel N60 (Kanto)]. ^{1}H NMR spectra were obtained on JEOL ECS400 spectrometer. ^{13}C NMR spectra were obtained on JEOL ECA500 spectrometers. Positive EI mass spectra was taken by using Shimadzu QP-5050 spectrometer. Data collection for X-ray crystal structure analyses for **1** were performed at 90 K and at 100 – 400 K with an interval of 50 K on RIGAKU AFC-8 diffractometer (Mo-Kα, λ = 0.71073 Å) equipped with a Saturn70 CCD detector. Details for X-ray electron density distribution analysis of **1** at 90 K is described below. Data collection for conventional X-ray crystal structure analyses for **2a** and **3** were performed at 150 K and 200 K, respectively, on a Rigaku/Varimax diffractometer (Mo-Kα, λ = 0.71075 Å). The structures were solved with a direct method and refined with a full-matrix least squares method. Raman spectra were recorded on JASCO NRS-3100T spectrometer.

9,9'-((9*H*-fluoren-9-ylidene)methylene)bis(9*H*-fluorene) (2): 9-(dibromomethylene)-9*H*-fluorene (332 mg, 0.988 mmol), fluorene (598 mg, 3.60 mmol), and dried NaO^{t}Bu were added to 1,3-dimethyl-2-imidazolidinone (DMI, 10 ml). After stirring for 24 h at room temperature, the reaction was quenched with water and the reaction mixture was extracted with dichloromethane (DCM). The combined organic layer was dried over Na_2SO_4 and evaporated in vacuo. The residue was purified by column chromatography on silica gel [DCM/*n*-hexane (1:9 *v*/*v*)] to give **2** (218 mg, 0.431 mmol, 43%) as colorless powder. **2** was obtained as a mixture of stereoisomers, **2a** and **2b**. **2a**: ^{1}H NMR (400 MHz, DMSO-d_6) δ 8.25 (d, J = 7.7 Hz, 2H), 8.13 (dd, J = 7.7, 1.0 Hz, 2H), 7.50 (t, J = 7.4 Hz, 2H), 7.38 (d, J = 7.7 Hz, 4H), 7.33 (dt, J = 7.7, 1.1 Hz, 2H), 7.15 (t, J = 7.4 Hz, 4H), 6.84 (dt, J = 7.4, 1.0 Hz, 4H), 6.70 (d, J = 7.7 Hz, 4H), 6.05 (s, 2H); ^{13}C NMR (126 MHz, DMSO-d_6) δ 146.9, 143.0, 141.3, 140.0, 138.8, 137.9, 128.1, 127.9, 126.6, 126.3, 125.8, 125.2, 120.0, 119.5, 51.9; EI-MS *m*/*z* 506 (M^+); analysis (calcd., found for $C_{40}H_{26}$): C (94.83, 94.80), H(5.17, 5.38). **2b**: ^{1}H NMR (400 MHz, DMSO-d_6) δ 8.51 (d, J = 6.7 Hz, 2H), 7.96 (dd, J = 6.2, 1.8 Hz, 2H), 7.66–7.59 (m, 4H), 7.56 (d, J = 7.3 Hz, 2H), 7.45 (d, J = 7.3 Hz, 2H), 7.15 (dt, J = 7.4, 1.1 Hz, 2H), 6.96 (dt, J = 7.4, 0.6 Hz, 2H), 6.89 (dt, J = 7.6, 1.2 Hz, 4H), 6.49 (dt, J = 7.6, 1.2 Hz, 2H), 6.26 (d, J = 7.8 Hz, 2H), 5.83 (s, 2H), 5.21 (d, J = 7.8 Hz, 2H); ^{13}C NMR (126 MHz, DMSO-d_6) δ 145.9, 143.6, 143.2, 142.8, 141.2, 140.7, 128.1, 127.7, 127.4, 127.2, 126.9, 126.2, 125.7, 123.9, 122.9, 120.4, 119.6, 119.1, 52.2; EI-MS *m*/*z* 506 (M^+); analysis (calcd., found for $C_{40}H_{26}$): C (94.83, 94.71), H(5.17, 5.44).

Tris(9-fluorenylidene)methane (1): In an argon-filled Schleck tube, *n*-butyllithium (1.8 M in hexane, 0.1 ml, 0.18 mmol) was added to a solution of compound **2** (32 mg, 0.063 mmol) in degassed THF (4.0 ml) at room temperature. The reaction mixture was stirred for 30 min to afford a deep-purple solution. A solution of *p*-chloranil (23.6 mg, 0.096 mmol) in degassed THF

(2 ml) was added slowly to the reaction mixture. The reaction mixture was allowed to stand for two days at room temperature. The resulting deep purple crystals were collected by filtration and washed with DCM and ethanol to give **1** (8 mg, 0.016 mmol, 27%). CP/MAS ^{13}C NMR (100 MHz, powder, 100 K) δ 143.6, 141.1, 132.4, 130.5, 128.1, 124.9, 122.2, 119.8, 82.9; (200 K) δ 141.1, 140.1, 137.0, 132.0, 130.1, 128.2, 124.7, 122.5, 119.7, 80.1; (300 K) δ 141.2, 140.3, 137.5, 131.9, 129.9, 128.6, 124.8, 122.8, 121.3, 120.0, 79.5.

Isolation of tris(9-fluorenylidene)methane dianion (3) in crystalline form: In a argon-filled Schlenk tube, *n*-butyllithium (1.8 M in hexane, 0.2 ml, 0.36 mmol) was added to a solution of compound **2** (53 mg, 0.105 mmol) in THF (4.0 mL) at room temperature. The reaction mixture was stirred for 30 min to afford a deep-purple solution. *n*-Hexane (4.0 ml) was slowly added to the reaction mixture and allowed to stand for 2 days. A trace amount of deep purple crystals was collected under argon atmosphere. ^{1}H NMR (400 MHz, THF-d_8) δ 8.01 (d, J = 7.4 Hz, 6H), 6.95 (d, J =7.4 Hz, 6H), 6.66 (dt, J = 7.4, 1.1 Hz, 6H), 6.56 (dt, J = 7.4, 1.1 Hz, 6H); ^{13}C NMR (100 MHz, THF-d_8) δ 143.9, 141.0, 130.1, 121.54, 121.1, 117.4, 113.1, 108.8.

Methods

Computational details: All quantum chemical calculations were performed with the Gaussian 16 program, revision B.01 [S1]. Version 3.8 of the multiwfn software [S2] was used for topological analysis of the electron density that is obtained by DFT calculations.

Polarized reflectivity spectra and their analyses: Steady-state reflectivity (R) spectra for 1.5–5.7 eV were measured by using a microscopic spectrometer (MSV 5200TSO, JASCO) equipped with a specially designed cryostat. Fig. S10A shows the R spectra of 1 at 100 K obtained with light polarized along (red solid line) and perpendicular (black solid line) to the a-axis on the single crystal (001) face. We obtained the optical conductivity (σ) spectra from the R spectra using the Kramers-Kronig transformation, which are shown in Fig. 2A in the main paper. In Fig. S10B and S10C, we show respectively the polarized R and σ spectra along the a-axis at 100 K, 200 K and 300 K. The temperature dependence of the peak wavelength corresponding to the HOMO to LUMO transition of **1** is plotted in nm in Fig. S10D, which is also shown in Fig. 4d. The peak wavelength of each σ spectrum shown in Fig. S10D is obtained from the fitting analyses, in which a Gaussian spectral shape is assumed to reproduce each peak or shoulder structure of the σ spectra below 2.5 eV. Error bars are determined, taking into account the standard deviations of the least-squares fit.

X-ray electron density distribution analysis of 1: A purple block shaped single crystal of **1**, 0.14 × 0.10 × 0.05 mm^3, was selected for measurements. The diffraction data were collected using a RIGAKU AFC-8 diffractometer equipped with a Saturn70 CCD detector with Mo$K\alpha$ radiation by an oscillation method about the ω-axis at 90 K. X-rays were monochromated and focused by a confocal mirror. Bragg spots were integrated, scaled and averaged up to $\sin\theta / \lambda$ = 1.11 Å^{-1} by the program HKL2000 [S3]. Lorentz and polarization, but no absorption corrections were applied. The number of measured and independent reflections, completeness, and $R_{\rm int}$ were 151624, 28858, 0.993 and 0.0332, respectively, up to $\sin\theta / \lambda$ = 1.11 Å^{-1}.

The initial structure of **1** was solved by a dual-space method using the program SHELXT-2018/2 [S4] and refined by a full matrix least-squares method using the program SHELXL-2018/3 [S4]. Positions of all hydrogen atoms were located on difference Fourier maps and refined by applying riding models.

High order refinements were carried out using 24397 independent reflections with $\sin\theta/\lambda \geq 0.60$ Å^{-1}, which is enough to avoid the contribution of valence electrons on the diffraction data (Fig. S1). The C–H distance was constrained at 1.083 Å during the refinements.

The multipole refinements using the Hansen-Coppens multipole formalism [S5] and topological analysis based on the resulted parameters were performed with the XD2006 package [S6]. The refinements were carried out against 19007 inependent reflections with $\sin\theta/\lambda \leq 1.11$ Å^{-1} with $I > 3\sigma(I)$ based on F^2. At the first stage of the refinements, the atomic coordinates and temperature factors of the atoms were fixed on those from the high order refinement. The population parameters, P_v, $P_{lm\pm}$ of the non-hydrogen atoms and scale were refined. The multipole level of population parameters was raised up to hexadecapole for the carbon atoms of central and fluorenyl 9*H*-position and octupole for the other carbon atoms, and dipole along the C−H bonds for hydrogen atoms. Chemical equivalent constraints were imposed for multipole parameters of all atoms. The radial screening parameters, κ and κ' were refined after refinements of multipole parameters at the highest level of each atom. The refinement cycles were repeated until parameters converged. At the second stage, the temperature factors were refined by applying harmonic anisotropic models for the non-hydrogen atoms, and isotropic models for hydrogen atoms, following the refinements of the radial screening parameters, κ and κ'. The chemical equivalent constraints on the multipole parameters were relaxed in a stepwise manner until releasing all the constraints on the C-atoms. The stage was repeated until the shifts of the parameters converged. At the final stage, the coordinates, temperature factors, and multipoles were refined. The C−H distances were constrained at 1.083. The number of parameters at the final cycle of the refinements was 1116. Total molecular charge was constrained to be neutral.

Solid-state NMR spectroscopy of 1: One-dimensional ^{13}C CP-MAS NMR experiments were performed using JEOL ECA400 spectrometer. The typical ^{1}H pulse width was 2.75 μs, and the contact time for CP was 7 ms. The relaxation delay was 5 s, and the spectral width was 40.2 kHz. For ^{1}H decoupling, the TPPM pulse sequence was used and the strength was 90.9 kHz. Spectra were recorded at 100 K, 200 K, and 300K under 10 kHz MAS.

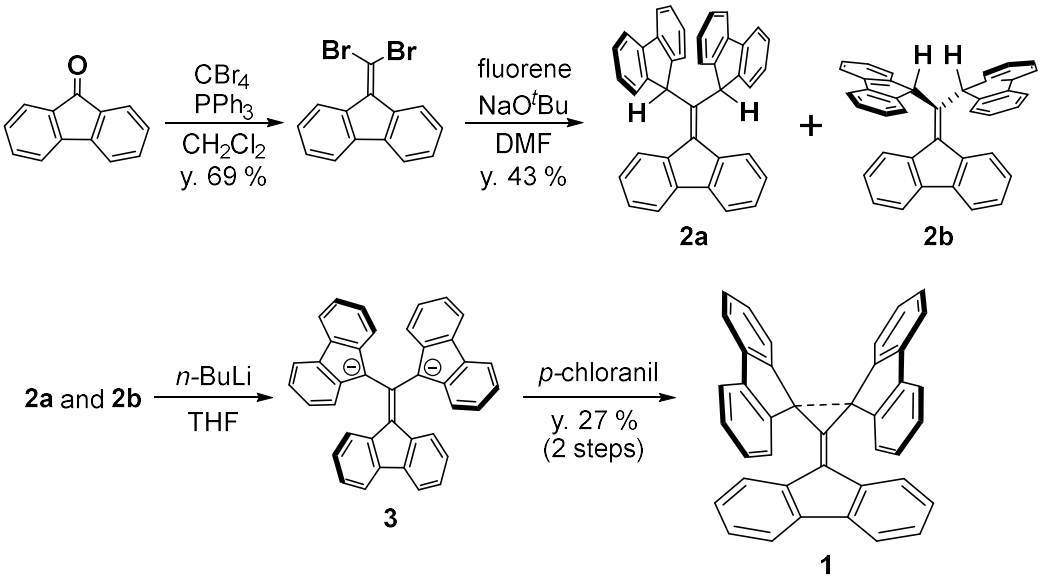

Scheme S1.

Synthetic route to **1**. The structure of **2a** was confirmed by $^{1}H/^{13}C$ NMR and X-ray structural analyses. As for **2b**, a proposed structure is shown, which is based on ^{1}H and ^{13}C NMR analyses.

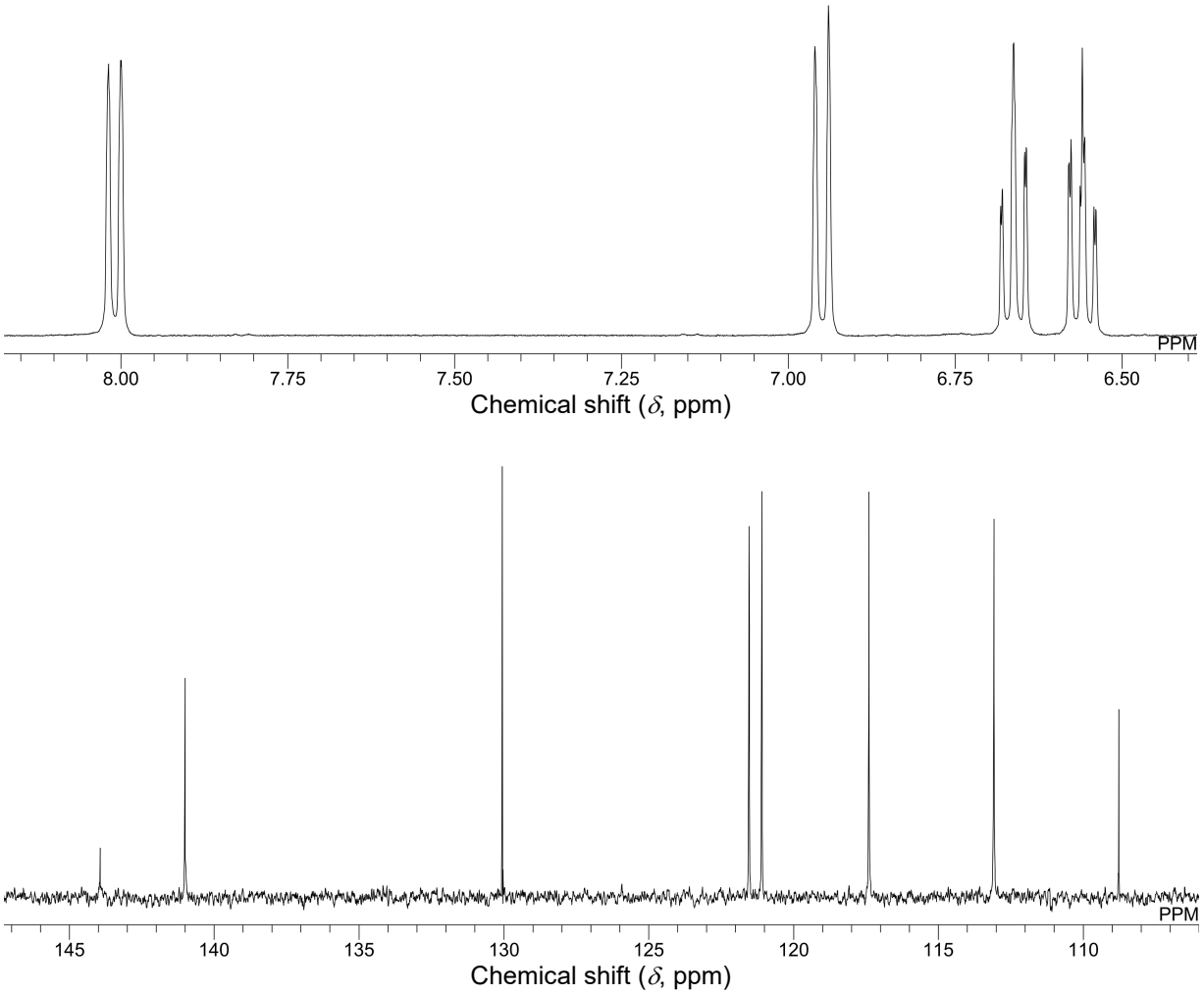

Fig. S1.
(Top) ^{1}H NMR and (bottom) ^{13}C NMR spectra of dianion species (**3**) in THF-d_8 measured at room temperature.

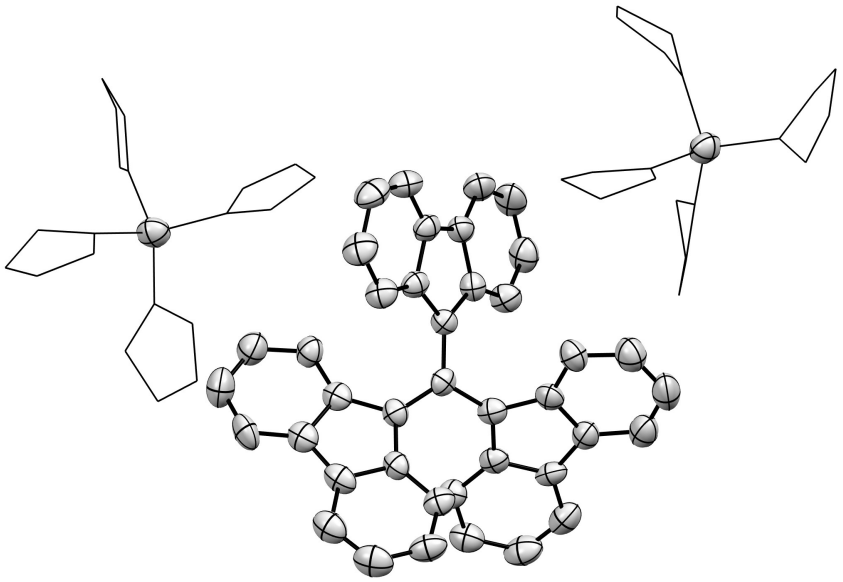

Fig. S2.
ORTEP drawing of **3**•$[Li(THF)_4]_2$. Thermal ellipsoids are drawn at the 50% probability level. Hydrogen atoms are omitted for clarity. THF molecules coordinated to a lithium cation atom are drawn with a wireframe model.

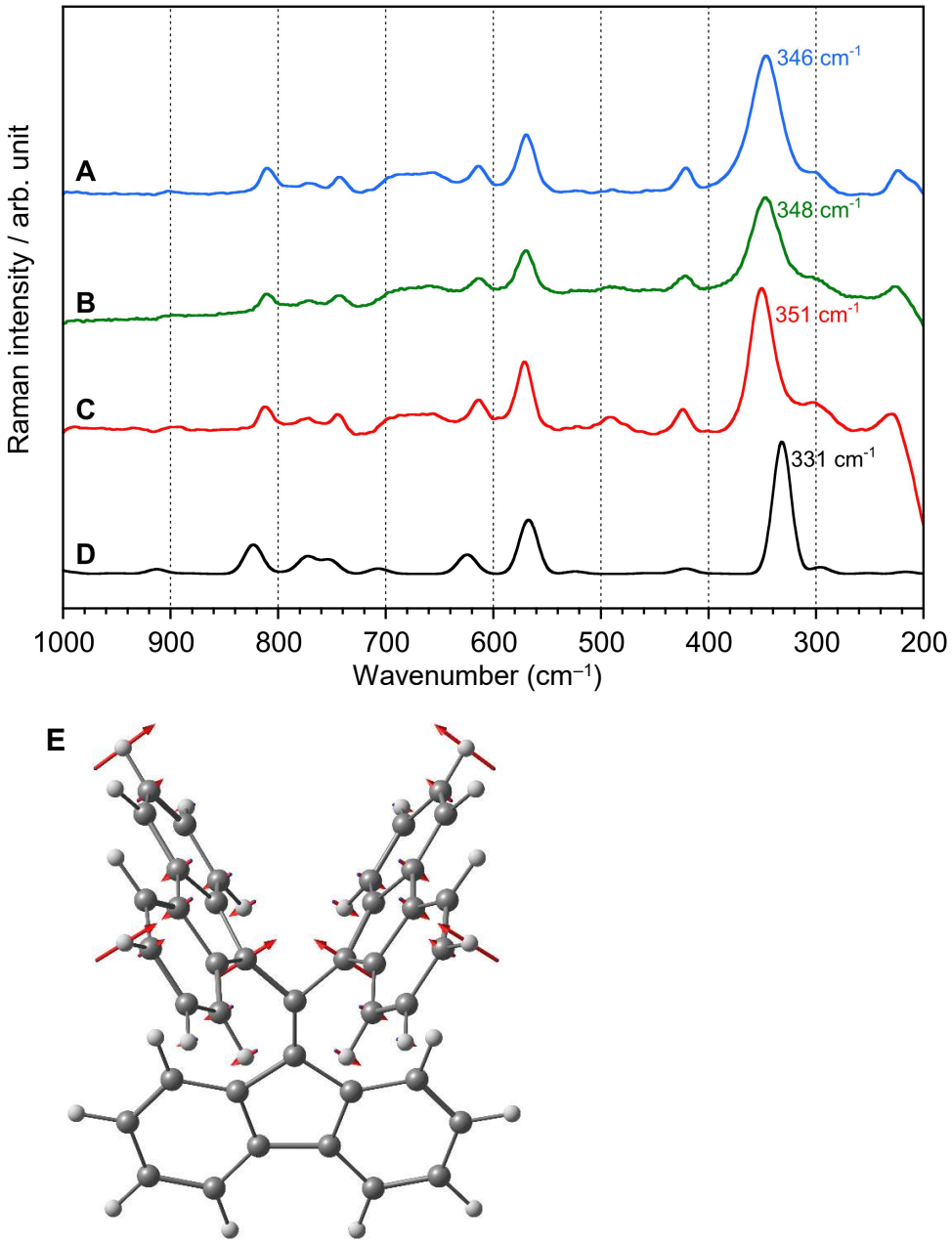

Fig. S3.

Experimental and theoretical Raman vibrational spectra of **1**. (A) Measured with a single crystal at 300 K, (B) 200 K, and (C) 100 K. (D) Simulated by the B3LYP-D3/6-311+G** calculation with the geometry optimized by the B3LYP-D3/6-311+G** calculation. All calculated states were broadened with a Gaussian of 20 cm^{-1} full width at half maximum. According to the B3LYP-D3 calculation, the peak of 331 cm^{-1} corresponds to the C2–C3 stretching vibration. However, the contribution weight of the Raman active C2–C3 stretching vibration to the peak of 331 cm^{-1} is only 8.0%: a scissoring motion of the bisfluorenylmethylidene moiety dominates the peak (see Fig. E).

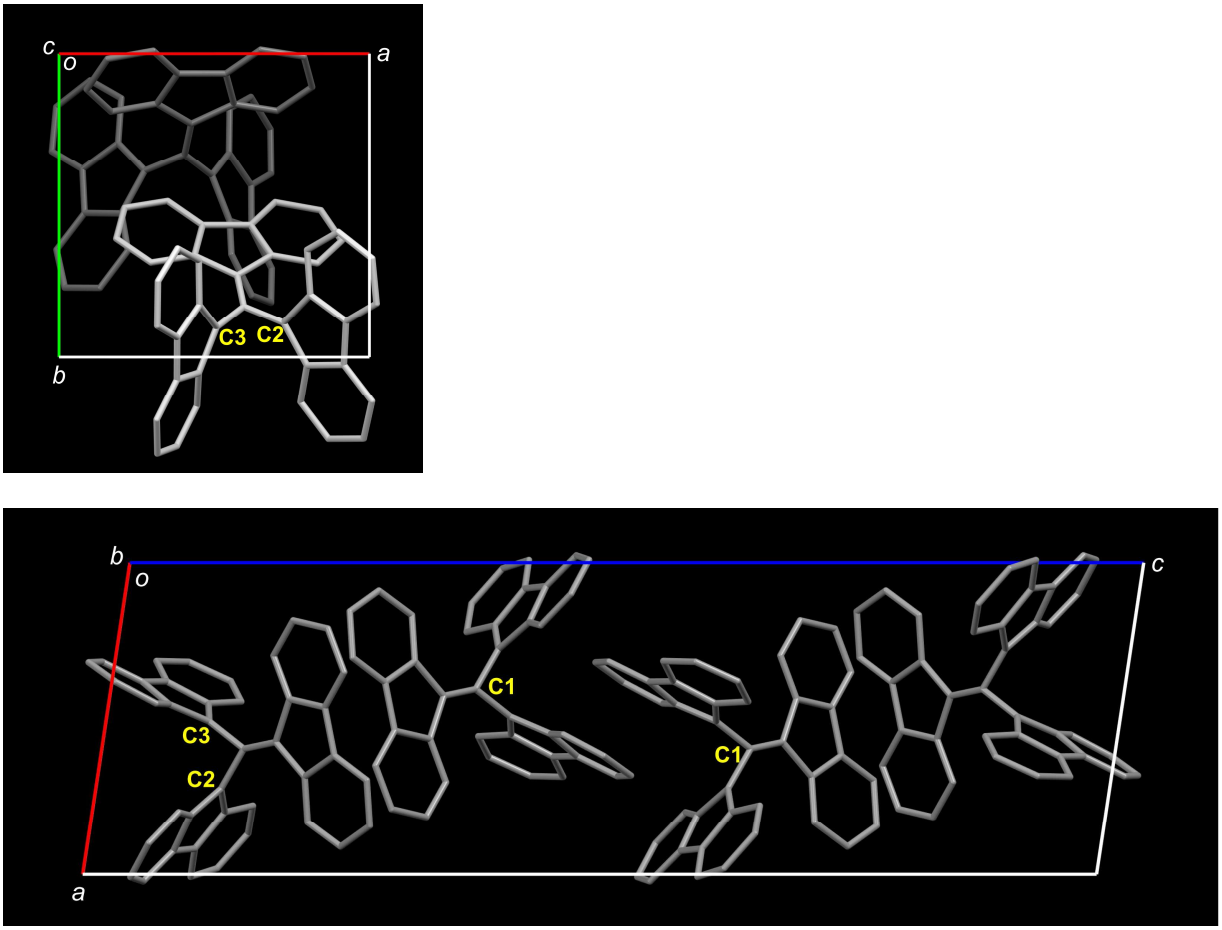

Fig. S4.

Crystal packing diagram of **1** along (top) *c*-axis and (bottom) *b*-axis. Hydrogen atoms are omitted for clarity.

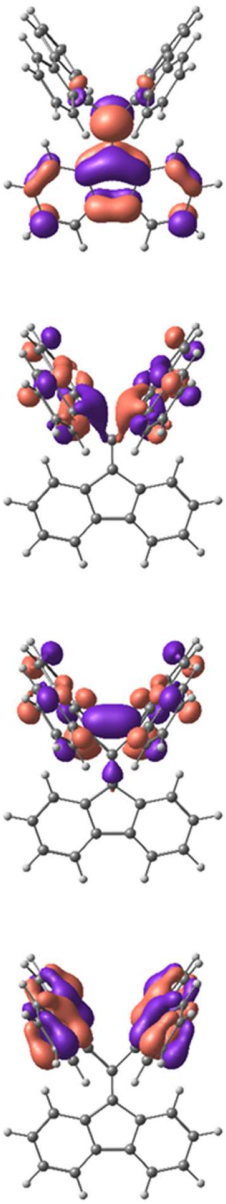

Fig. S5.

TD-B3LYP-D3/6-311+G** calculation results of **1**. The structure used for the TD calculation was optimized at the B3LYP-D3/6-311+G** level of theory and converged to the C_s symmetry. The peak of 518 nm observed at 100 K corresponds to $S_0 \rightarrow S_3$ transition.

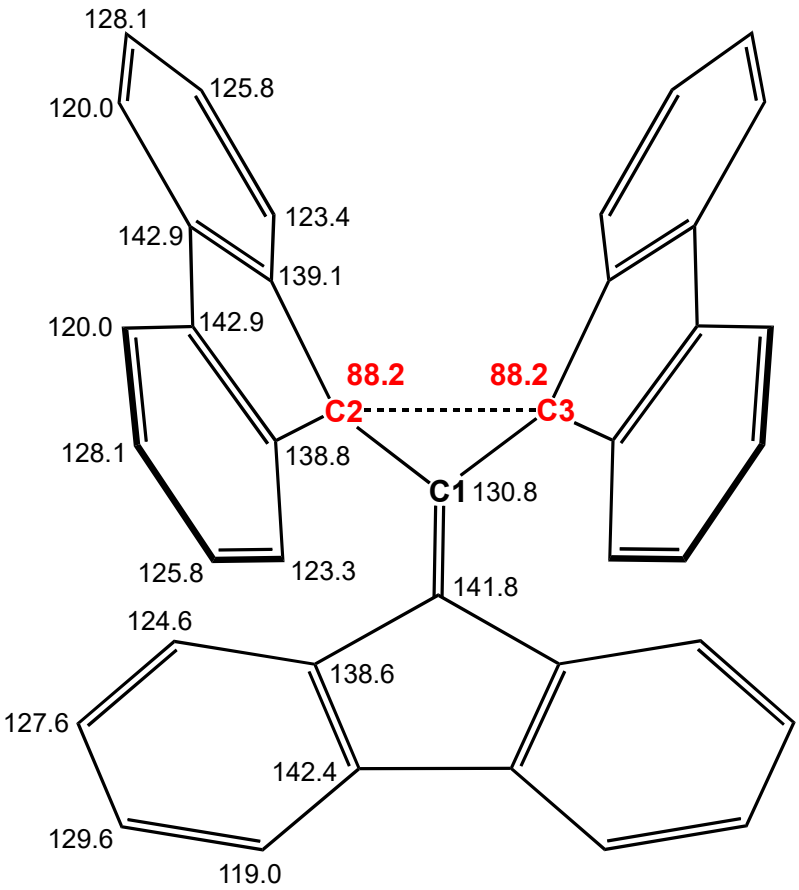

Fig. S6.

Theoretically predicted ^{13}C chemical shifts (δ_{pred}) of **1**, which was estimated by the empirically scaled GIAO-B3LYP-D3/6-311+G** method. The structure was optimized at the B3LYP-D3/6-311+G** level of theory and converged to the C_s symmetry. The following equation was applied to the GIAO-calculated chemical shifts (δ_{GIAO}); $\delta_{pred} = (181.3782 - \delta_{GIAO}) / 1.0228$ [S7].

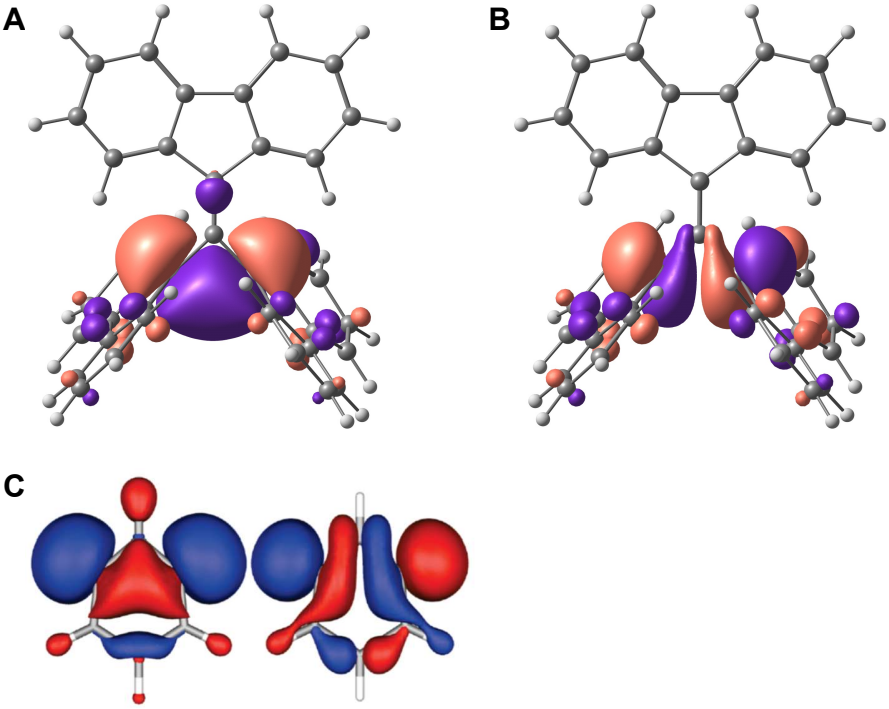

Fig. S7.

(A) HONO and (B) LUNO of **1** plotted with an isodensity value of 0.03 e au^{-3}. (C) TCSCF orbitals ψ_S' and ψ_A' of *m*-benzyne. Reprinted with permission from Wei, H.; Hrovat, D. A.; Mo, Y.; Hoffmann, R.; Borden, W. T. *J. Phys. Chem. A* **113**, 10351–10358 (2009). Copyright 2009 American Chemical Society.

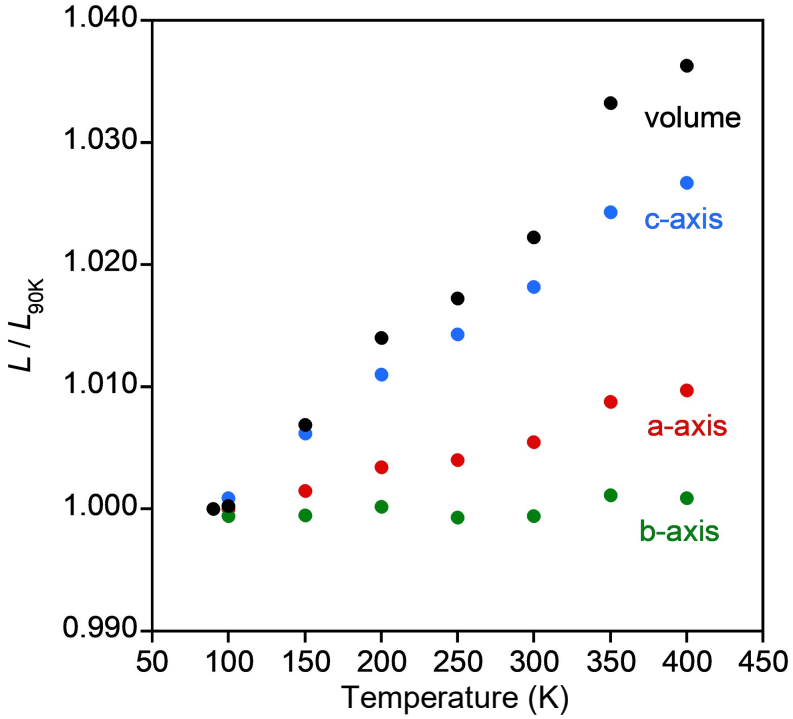

Fig. S8.

Temperature dependence of the lattice parameters (L) for **1**.

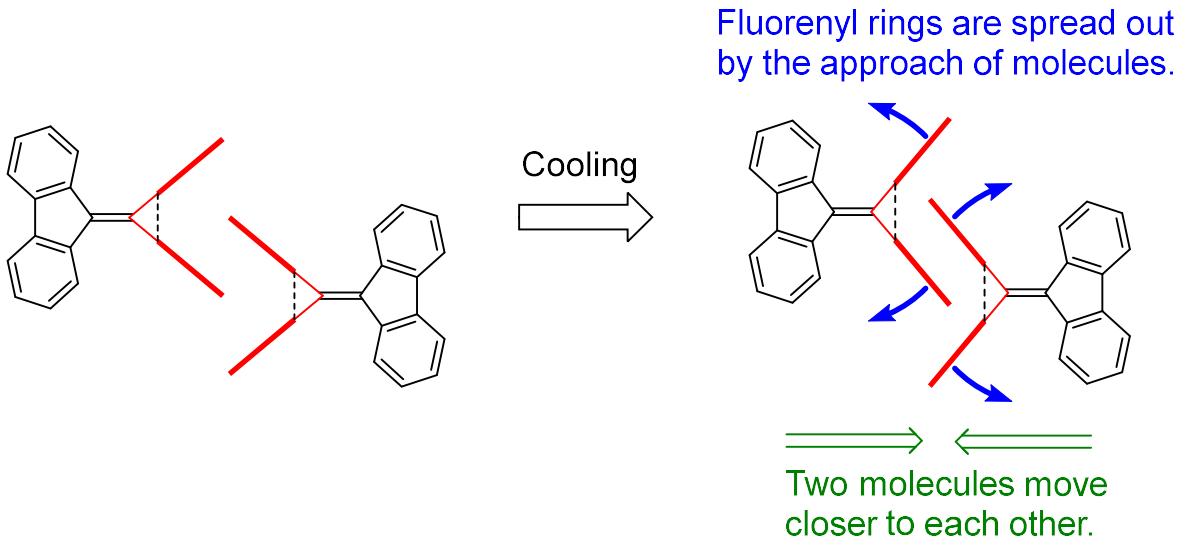

Fig. S9.

Schematic drawing for the effect of the interlocked dimeric structure of **1** on the interatomic distance between C2 and C3.

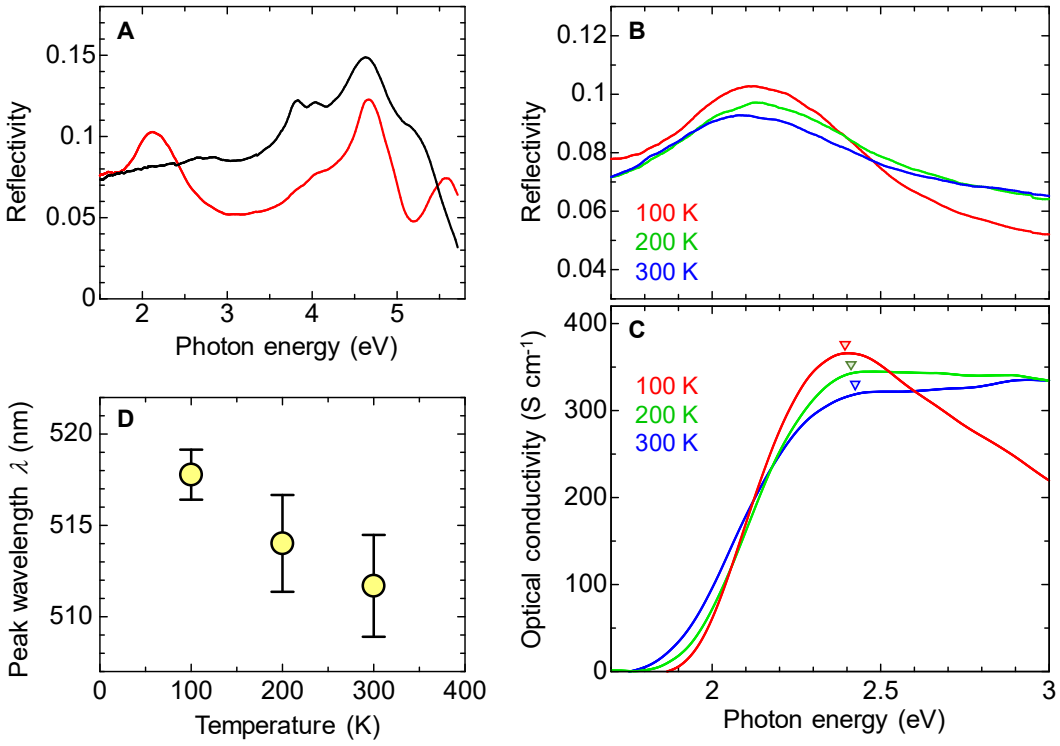

Fig. S10.

(A) Optical reflectivity (R) spectra of **1** at 100 K obtained with light polarized along (red solid line) and perpendicular (black solid line) to the a-axis on the single crystal (001) face. (B) The R spectra and (C) the σ spectra of **1** along the a-axis at 100 K, 200 K, and 300 K in the visible region. (D) The temperature dependence of the transition peak wavelength of the σ spectra shown by the triangles in Fig. C.

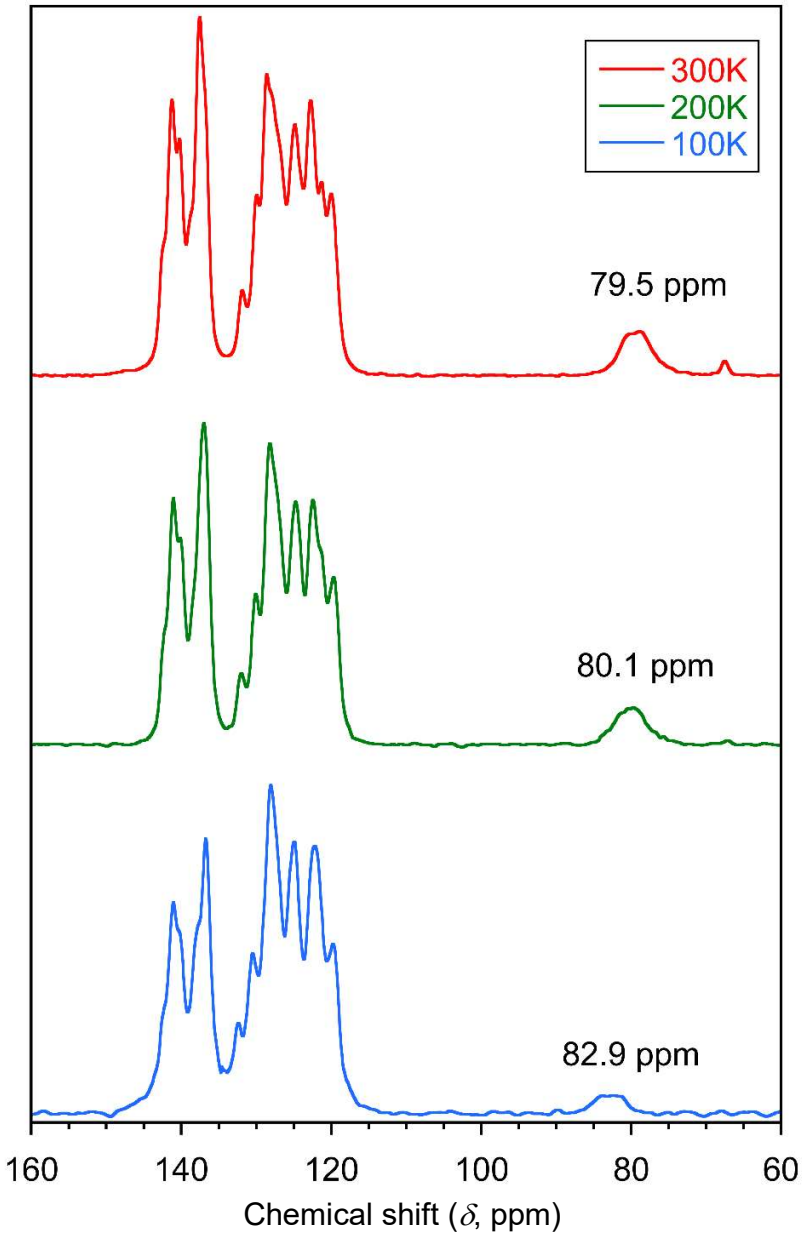

Fig. S11.

Solid state CP/MAS ^{13}C NMR spectra of powdered **1** measured at 100, 200, and 300 K. Chemical shifts are referenced to the methyl carbon (δ 17.17) of hexamethylbenzene as a standard.

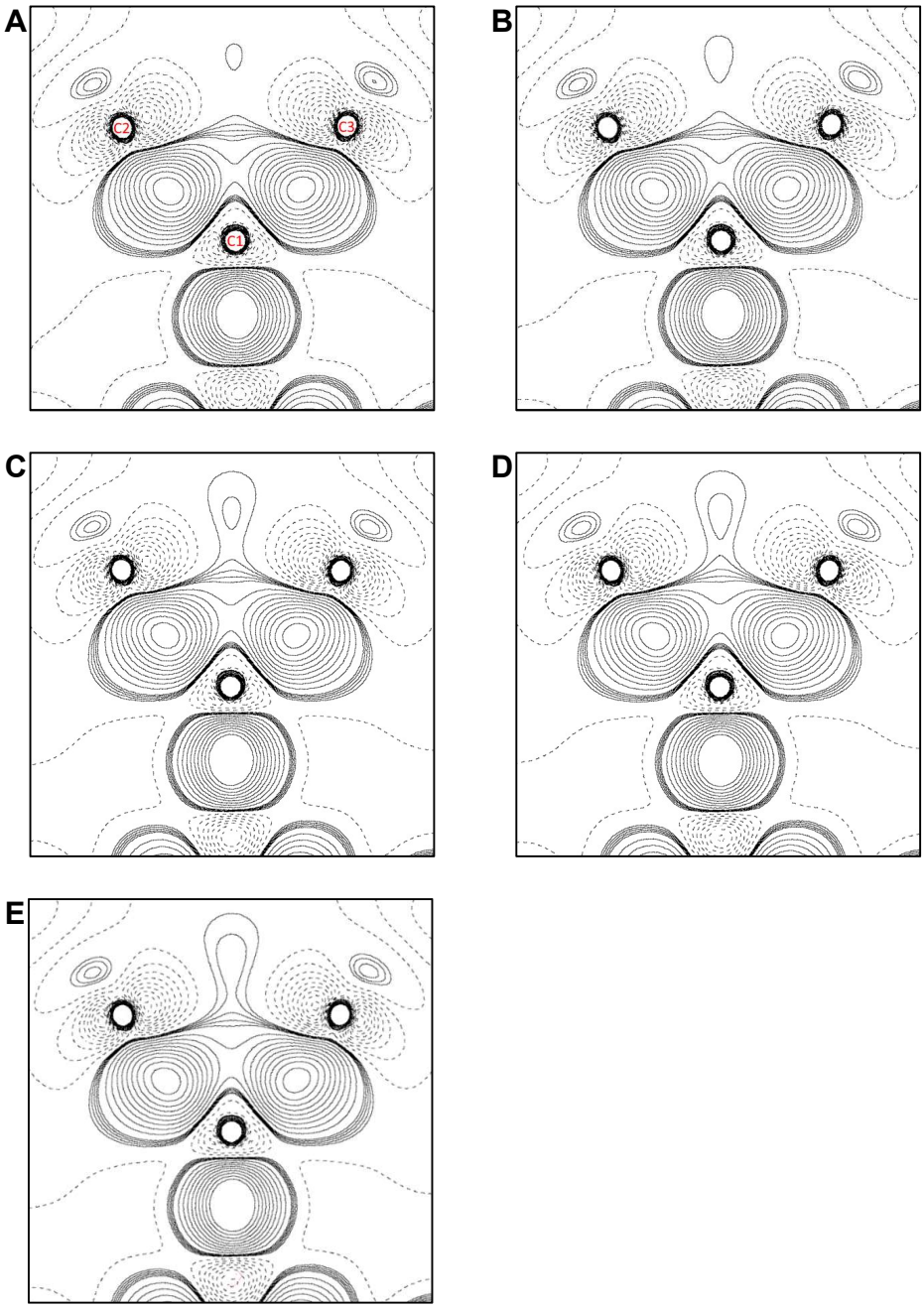

Fig. S12.

Static model deformation density maps on the C1-C2-C3 plane of **1**, obtained by the B3LYP-D3/6-311+G** calculation. The molecular structures used for the calculation are based on the X-ray crystallographic measurements at (A) 90 K, (B) 100K, (C) 200 K, (D) 300 K, and (E) 400K. The solid lines represent positive contours from 0.01 to 0.05 e $Å^{-3}$ in steps of 0.01 e $Å^{-3}$ and from 0.10 to 0.50 e $Å^{-3}$ in steps of 0.05 e $Å^{-3}$. The dashed lines represent negative contours from –0.05 to –0.50 in steps of –0.05 e $Å^{-3}$.

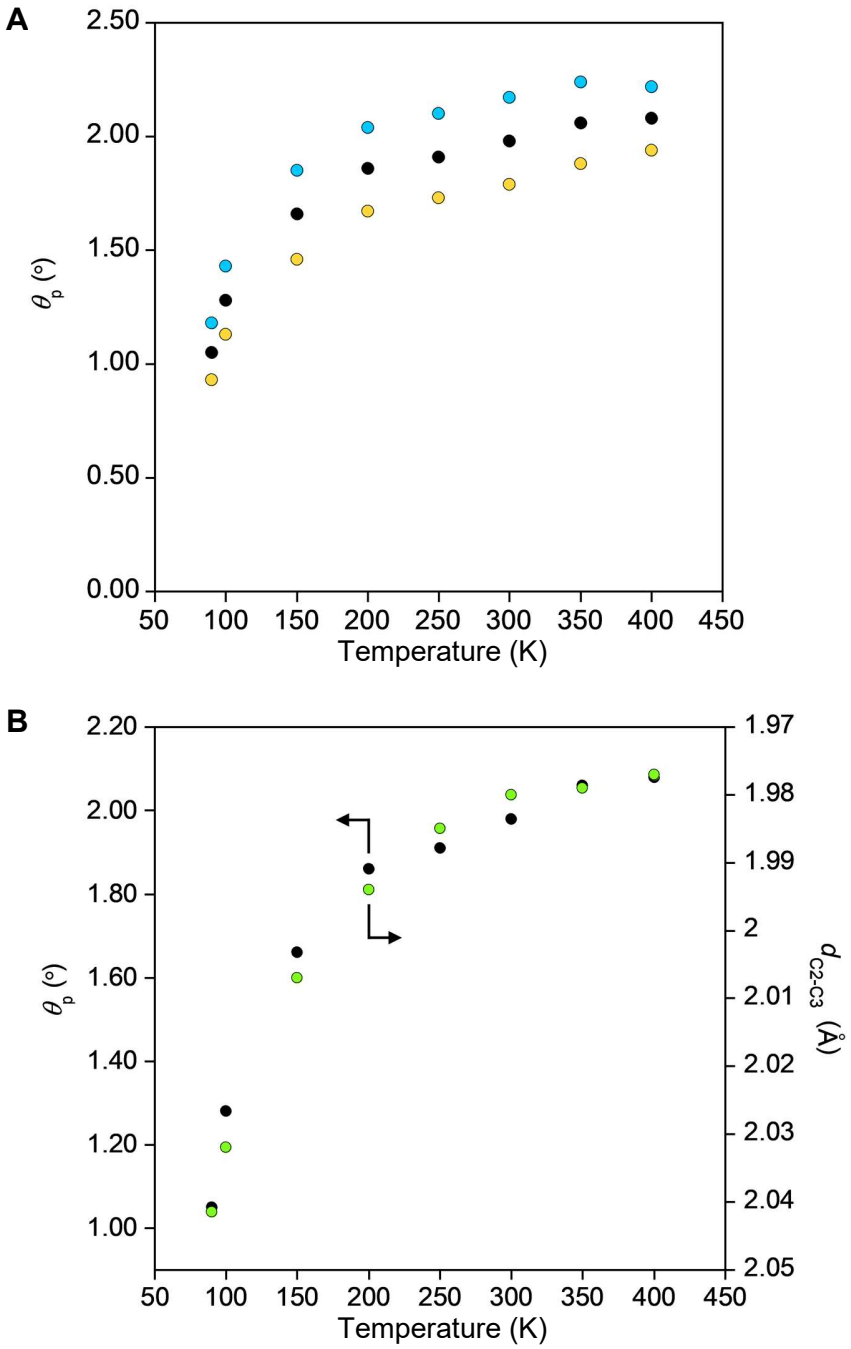

Fig. S13.

(A) Temperature dependence of the pyramidalization angle (θ_p, °) of C2 and C3 determined by the POAV analysis. (B) Comparison of the temperature dependence of θ_p with that of $d_{C2–C3}$.

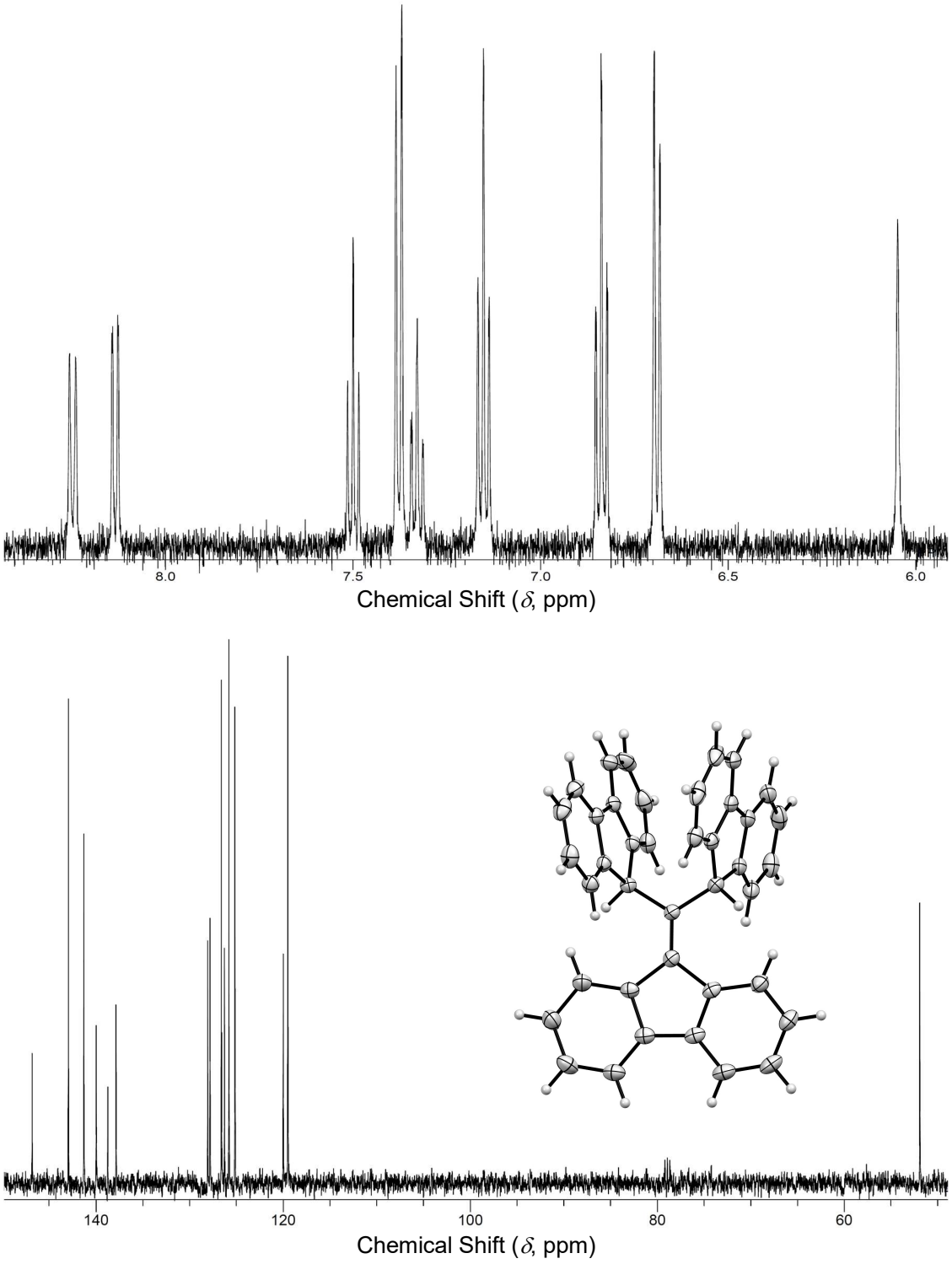

Fig. S14.

(Top) ^{1}H and (bottom) ^{13}C NMR spectra of **2a** in DMSO-d_6. The structure of **2a** was confirmed by X-ray crystallographic analysis, as shown as the ORTEP drawing.

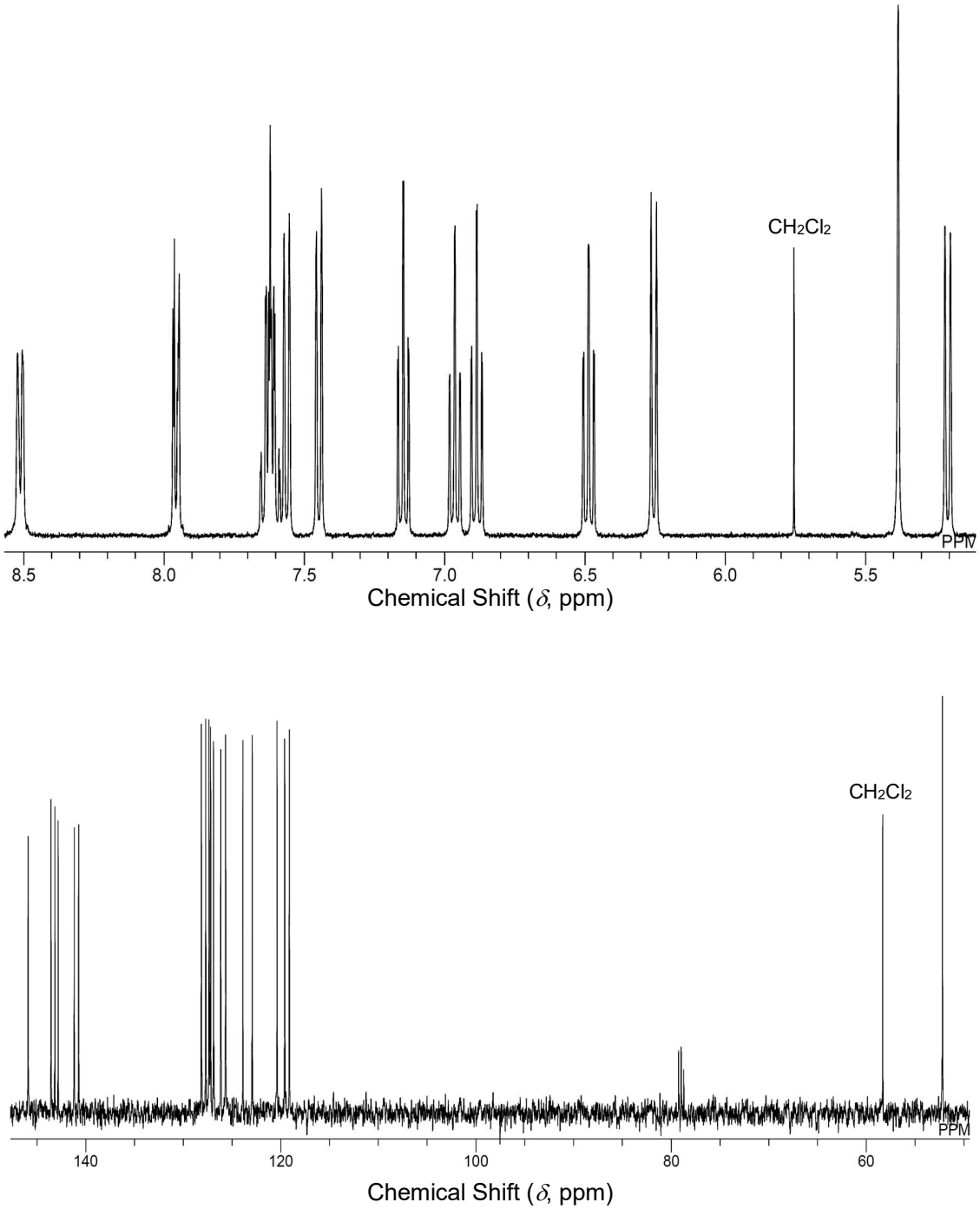

Fig. S15.
(Top) ^{1}H and (bottom) ^{13}C NMR spectra of **2b** in DMSO-d_6.

Table S1.

Equilibrium structures of **1** calculated at different DFT levels of theory [a].

DFT method	Basis set	Interatomic distance [b] ($d_{C2–C3}$) / Å	Bond angle [b] ($\theta_{C2\text{-}C1\text{-}C3}$) / °	Sum of electronic and zero-point energies / hartree
B3LYP	6-31G*	1.791	75.89	−1538.195923
B3LYP	6-31G**	1.794	76.01	−1538.234577
B3LYP	6-311G**	1.810	76.90	−1538.539168
B3LYP-D3	6-31G*	1.801	76.69	−1538.270365
B3LYP-D3	6-31G**	1.804	76.86	−1538.309033
B3LYP-D3	6-31+G**	1.802	76.70	−1538.356385
B3LYP-D3	6-311G*	2.047	89.25	−1538.571220
B3LYP-D3	6-311G**	2.048	89.33	−1538.614029
B3LYP-D3	6-311+G**	2.048	89.32	−1538.628896
B3LYP-D3	cc-pVDZ	2.071	90.20	−1538.361481
B3LYP-D3	cc-pVTZ	2.043	89.27	−1538.769782
B3LYP-D3(BJ)	6-31G*	2.108	92.42	−1538.377889
B3LYP-D3(BJ)	cc-pVTZ	2.100	92.26	−1538.877506
B3PW91-D3	6-311G*	1.726	73.17	−1537.974350
B3PW91-D3(BJ)	6-311G*	1.718	72.91	−1538.078416
B3PW91-D3	cc-pVTZ	1.725	73.30	−1538.169009
M06-2X	6-311G*	1.656	69.41	−1537.889563
M06-2X	cc-pVTZ	1.653	69.44	−1538.088938
wB97XD	6-311G*	1.668	70.08	−1537.965158
wB97XD	cc-pVTZ	1.666	70.18	−1538.150041
PBE0-D3	6-311G*	1.696	71.67	−1536.719217
PBE0-D3(BJ)	6-311G*	1.692	71.53	−1536.769500

[a] Frequency calculation was performed for each optimized structure to ensure that a minimum on the potential energy surface was located.

[b] The interatomic distances and bond angles are diverse and strongly depend on the level of theory applied. Similar findings have been reported for *m*-benzyne [S8].

Summary of DFT calculations.

Cartesian coordinates used for DFT calculations (NBO analysis, singlet–triplet energy gap, electron density analysis, and CASSCF calculations).

1 at 90 K

6	0.000000000	0.000000000	0.000000000
6	1.316060507	0.267307895	0.027824991
6	2.168627929	0.348282272	1.230398458
6	1.867761193	0.149927037	2.576661213
6	2.908302949	0.212815708	3.509507861
6	4.220787584	0.489261749	3.105108712
6	4.524966042	0.692855302	1.756090502
6	3.494596670	0.610550520	0.822510896
6	3.516417689	0.711344313	-0.642853719
6	4.562158897	0.967681658	-1.524747983
6	4.284792680	1.005925325	-2.895929373
6	2.987504097	0.783695982	-3.374386741
6	1.933461434	0.536123349	-2.491977054
6	2.206943542	0.499429020	-1.124333072
6	-1.035576413	0.000000000	-1.018177536
6	-1.586195649	1.187238770	-1.688979712
6	-1.180950468	2.521791452	-1.682857352
6	-1.871370339	3.435824663	-2.489433256
6	-2.957943527	3.032053335	-3.271703939
6	-3.339801559	1.687743341	-3.311454207
6	-2.638085842	0.770865337	-2.544252291
6	-2.711583460	-0.688710551	-2.511998192
6	-3.501423102	-1.568774199	-3.242107305
6	-3.253534018	-2.941929607	-3.123464035
6	-2.202907964	-3.411662160	-2.328395973
6	-1.403087037	-2.522911869	-1.593003286
6	-1.691441280	-1.159319266	-1.642003727
6	-1.035576413	0.000000000	1.022865335
6	-1.750938336	-1.118504871	1.649200048
6	-1.614810336	-2.503925951	1.526731283
6	-2.475596160	-3.335838691	2.255646888
6	-3.427879657	-2.794584319	3.130117496
6	-3.519041714	-1.412009772	3.319001329
6	-2.682316402	-0.586790867	2.582193679
6	-2.521150930	0.865877906	2.626206474
6	-3.148612475	1.831561978	3.408502634
6	-2.720483875	3.161478287	3.305204460
6	-1.669223234	3.503476274	2.450527655
6	-1.045057497	2.537905000	1.648153524
6	-1.495024545	1.217828575	1.711611280
1	0.852084935	-0.049978498	2.893920596
1	2.696963466	0.046592516	4.558109060

1	5.008503059	0.543403286	3.845569396
1	5.538024352	0.911698981	1.445194534
1	5.568206599	1.136379395	-1.159856088
1	5.086024988	1.210453274	-3.596778934
1	2.800891177	0.804526877	-4.440959144
1	0.927838767	0.376974482	-2.861068762
1	-0.350059235	2.844244975	-1.067062349
1	-1.558029067	4.472331307	-2.507851292
1	-3.506602838	3.764952945	-3.850500209
1	-4.170329739	1.370006476	-3.929822404
1	-4.291138580	-1.202370936	-3.886640557
1	-3.880786411	-3.647668838	-3.654110409
1	-2.005500116	-4.475872478	-2.279370055
1	-0.576843097	-2.890713368	-0.997954540
1	-0.856126534	-2.927698371	0.879540565
1	-2.406937846	-4.411372911	2.142557642
1	-4.098730559	-3.456257166	3.666245382
1	-4.228185981	-0.996868577	4.024203567
1	-3.951370085	1.561301845	4.083085230
1	-3.209323678	3.929228506	3.892700204
1	-1.331276693	4.530968827	2.409342827
1	-0.228746980	2.812441076	0.991093342

1 at 100K

6	2.175000000	3.022000000	10.771000000
6	2.514000000	2.101000000	9.865000000
6	1.623000000	1.496000000	8.849000000
6	0.285000000	1.732000000	8.559000000
1	-0.228000000	2.335000000	9.084000000
6	-0.285000000	1.064000000	7.477000000
1	-1.194000000	1.225000000	7.255000000
6	0.455000000	0.169000000	6.719000000
1	0.041000000	-0.283000000	5.993000000
6	1.793000000	-0.078000000	7.007000000
1	2.295000000	-0.695000000	6.488000000
6	2.377000000	0.598000000	8.070000000
6	3.762000000	0.600000000	8.569000000
6	4.880000000	-0.112000000	8.158000000
1	4.827000000	-0.726000000	7.435000000
6	6.079000000	0.094000000	8.826000000
1	6.851000000	-0.391000000	8.559000000
6	6.171000000	0.998000000	9.882000000
1	7.005000000	1.131000000	10.316000000
6	5.053000000	1.709000000	10.307000000
1	5.111000000	2.319000000	11.034000000
6	3.849000000	1.506000000	9.644000000
6	2.822000000	3.644000000	11.917000000

6	3.157000000	2.982000000	13.186000000
6	3.121000000	1.643000000	13.565000000
1	2.797000000	0.980000000	12.967000000
6	3.569000000	1.294000000	14.841000000
1	3.561000000	0.382000000	15.106000000
6	4.027000000	2.261000000	15.727000000
1	4.288000000	2.009000000	16.605000000
6	4.105000000	3.595000000	15.341000000
1	4.435000000	4.253000000	15.941000000
6	3.695000000	3.945000000	14.067000000
6	3.812000000	5.216000000	13.350000000
6	4.368000000	6.425000000	13.736000000
1	4.659000000	6.561000000	14.629000000
6	4.490000000	7.438000000	12.785000000
1	4.839000000	8.283000000	13.042000000
6	4.108000000	7.224000000	11.467000000
1	4.225000000	7.917000000	10.827000000
6	3.554000000	6.004000000	11.070000000
1	3.317000000	5.855000000	10.162000000
6	3.353000000	5.013000000	12.024000000
6	0.898000000	3.511000000	11.275000000
6	0.217000000	4.797000000	11.051000000
6	0.536000000	5.893000000	10.255000000
1	1.316000000	5.888000000	9.712000000
6	-0.317000000	7.003000000	10.269000000
1	-0.094000000	7.771000000	9.757000000
6	-1.483000000	6.998000000	11.022000000
1	-2.038000000	7.769000000	11.032000000
6	-1.851000000	5.881000000	11.761000000
1	-2.666000000	5.869000000	12.250000000
6	-1.003000000	4.784000000	11.770000000
6	-1.165000000	3.470000000	12.394000000
6	-2.203000000	2.940000000	13.147000000
1	-2.947000000	3.478000000	13.391000000
6	-2.135000000	1.605000000	13.538000000
1	-2.832000000	1.233000000	14.066000000
6	-1.056000000	0.811000000	13.162000000
1	-1.038000000	-0.104000000	13.415000000
6	0.001000000	1.340000000	12.419000000
1	0.733000000	0.792000000	12.162000000
6	-0.037000000	2.686000000	12.060000000

1 at 200 K

6	2.132000000	3.016000000	10.875000000
6	2.475000000	2.111000000	9.956000000
6	1.588000000	1.514000000	8.935000000
6	0.255000000	1.746000000	8.643000000

1	-0.261000000	2.345000000	9.171000000
6	-0.312000000	1.085000000	7.562000000
1	-1.222000000	1.243000000	7.341000000
6	0.428000000	0.199000000	6.802000000
1	0.016000000	-0.248000000	6.073000000
6	1.761000000	-0.046000000	7.088000000
1	2.265000000	-0.658000000	6.564000000
6	2.345000000	0.622000000	8.154000000
6	3.726000000	0.623000000	8.656000000
6	4.850000000	-0.083000000	8.246000000
1	4.800000000	-0.695000000	7.520000000
6	6.042000000	0.122000000	8.914000000
1	6.817000000	-0.359000000	8.646000000
6	6.128000000	1.016000000	9.968000000
1	6.961000000	1.147000000	10.405000000
6	5.012000000	1.723000000	10.395000000
1	5.070000000	2.330000000	11.124000000
6	3.812000000	1.522000000	9.732000000
6	2.759000000	3.641000000	12.028000000
6	3.100000000	2.979000000	13.298000000
6	3.065000000	1.645000000	13.679000000
1	2.740000000	0.980000000	13.083000000
6	3.515000000	1.299000000	14.951000000
1	3.508000000	0.387000000	15.217000000
6	3.971000000	2.263000000	15.834000000
1	4.232000000	2.012000000	16.712000000
6	4.051000000	3.591000000	15.446000000
1	4.382000000	4.250000000	16.045000000
6	3.641000000	3.943000000	14.174000000
6	3.763000000	5.210000000	13.453000000
6	4.324000000	6.417000000	13.837000000
1	4.612000000	6.555000000	14.731000000
6	4.456000000	7.420000000	12.888000000
1	4.808000000	8.264000000	13.144000000
6	4.080000000	7.208000000	11.574000000
1	4.206000000	7.898000000	10.933000000
6	3.519000000	5.993000000	11.177000000
1	3.285000000	5.843000000	10.269000000
6	3.307000000	5.007000000	12.132000000
6	0.872000000	3.518000000	11.400000000
6	0.189000000	4.803000000	11.160000000
6	0.507000000	5.888000000	10.354000000
1	1.284000000	5.875000000	9.808000000
6	-0.343000000	7.000000000	10.363000000
1	-0.121000000	7.764000000	9.844000000
6	-1.504000000	7.001000000	11.120000000
1	-2.057000000	7.774000000	11.126000000

6	-1.869000000	5.899000000	11.863000000
1	-2.683000000	5.894000000	12.353000000
6	-1.026000000	4.798000000	11.880000000
6	-1.198000000	3.491000000	12.511000000
6	-2.241000000	2.964000000	13.260000000
1	-2.984000000	3.505000000	13.499000000
6	-2.184000000	1.638000000	13.653000000
1	-2.885000000	1.271000000	14.179000000
6	-1.111000000	0.841000000	13.287000000
1	-1.098000000	-0.073000000	13.544000000
6	-0.052000000	1.359000000	12.547000000
1	0.676000000	0.804000000	12.295000000
6	-0.075000000	2.700000000	12.184000000

1 at 300 K

6	2.106000000	3.015000000	10.954000000
6	2.451000000	2.123000000	10.024000000
6	1.569000000	1.532000000	9.001000000
6	0.240000000	1.762000000	8.708000000
1	-0.266000000	2.346000000	9.225000000
6	-0.321000000	1.104000000	7.627000000
1	-1.213000000	1.256000000	7.412000000
6	0.419000000	0.229000000	6.867000000
1	0.019000000	-0.205000000	6.148000000
6	1.741000000	-0.014000000	7.154000000
1	2.234000000	-0.612000000	6.640000000
6	2.326000000	0.648000000	8.218000000
6	3.705000000	0.649000000	8.721000000
6	4.830000000	-0.052000000	8.311000000
1	4.784000000	-0.648000000	7.599000000
6	6.015000000	0.152000000	8.981000000
1	6.775000000	-0.316000000	8.718000000
6	6.096000000	1.036000000	10.029000000
1	6.912000000	1.164000000	10.457000000
6	4.984000000	1.739000000	10.460000000
1	5.041000000	2.329000000	11.176000000
6	3.788000000	1.541000000	9.797000000
6	2.727000000	3.636000000	12.106000000
6	3.066000000	2.979000000	13.376000000
6	3.030000000	1.648000000	13.760000000
1	2.713000000	0.995000000	13.178000000
6	3.477000000	1.308000000	15.027000000
1	3.467000000	0.416000000	15.291000000
6	3.933000000	2.268000000	15.903000000
1	4.188000000	2.024000000	16.763000000
6	4.016000000	3.588000000	15.515000000
1	4.344000000	4.232000000	16.100000000

6	3.606000000	3.939000000	14.248000000
6	3.735000000	5.201000000	13.523000000
6	4.296000000	6.404000000	13.905000000
1	4.576000000	6.539000000	14.781000000
6	4.434000000	7.400000000	12.962000000
1	4.782000000	8.225000000	13.213000000
6	4.064000000	7.188000000	11.655000000
1	4.194000000	7.862000000	11.027000000
6	3.497000000	5.979000000	11.255000000
1	3.269000000	5.834000000	10.365000000
6	3.279000000	5.001000000	12.208000000
6	0.851000000	3.520000000	11.482000000
6	0.172000000	4.804000000	11.234000000
6	0.492000000	5.878000000	10.422000000
1	1.252000000	5.860000000	9.885000000
6	-0.355000000	6.989000000	10.429000000
1	-0.140000000	7.734000000	9.916000000
6	-1.508000000	6.994000000	11.187000000
1	-2.046000000	7.752000000	11.192000000
6	-1.875000000	5.906000000	11.931000000
1	-2.672000000	5.907000000	12.412000000
6	-1.038000000	4.806000000	11.954000000
6	-1.214000000	3.506000000	12.591000000
6	-2.257000000	2.980000000	13.338000000
1	-2.984000000	3.512000000	13.569000000
6	-2.205000000	1.664000000	13.733000000
1	-2.894000000	1.309000000	14.247000000
6	-1.143000000	0.869000000	13.375000000
1	-1.134000000	-0.025000000	13.631000000
6	-0.085000000	1.378000000	12.639000000
1	0.625000000	0.829000000	12.396000000
6	-0.097000000	2.712000000	12.270000000

Cartesian coordinates of 1 optimized by the B3LYP-D3/6-311+G calculation**

6	-0.003530000	0.000000000	-0.507953000
6	-0.003106000	-1.023919000	0.528286000
6	-0.003106000	1.023919000	0.528286000
6	-1.172106000	-1.630035000	1.165457000
6	-2.524212000	-1.581302000	0.833938000
6	-3.440827000	-2.278492000	1.625008000
6	-3.011968000	-3.027037000	2.723101000
6	-1.650531000	-3.123978000	3.032276000
6	-0.732976000	-2.438232000	2.248950000
6	0.730810000	-2.438428000	2.247105000
6	1.650216000	-3.124294000	3.028166000
6	3.010885000	-3.027557000	2.715566000
6	3.437126000	-2.279042000	1.616422000

6	2.518649000	-1.581722000	0.827636000
6	1.167374000	-1.630394000	1.162492000
6	-1.172106000	1.630034000	1.165457000
6	-2.524212000	1.581302000	0.833939000
6	-3.440826000	2.278492000	1.625009000
6	-3.011968000	3.027036000	2.723102000
6	-1.650531000	3.123978000	3.032277000
6	-0.732976000	2.438232000	2.248950000
6	0.730811000	2.438428000	2.247105000
6	1.650216000	3.124294000	3.028166000
6	3.010885000	3.027556000	2.715566000
6	3.437127000	2.279042000	1.616422000
6	2.518649000	1.581722000	0.827636000
6	1.167374000	1.630394000	1.162493000
6	-0.000927000	0.000000000	-1.846063000
6	0.000877000	-1.180369000	-2.732882000
6	0.000437000	-2.540070000	-2.436767000
6	0.002525000	-3.455385000	-3.491888000
6	0.005053000	-3.015588000	-4.819066000
6	0.005553000	-1.651583000	-5.120848000
6	0.003464000	-0.734909000	-4.074644000
6	0.003464000	0.734910000	-4.074644000
6	0.005553000	1.651583000	-5.120848000
6	0.005053000	3.015589000	-4.819066000
6	0.002525000	3.455385000	-3.491888000
6	0.000437000	2.540070000	-2.436767000
6	0.000877000	1.180369000	-2.732882000
1	-2.857481000	-1.046483000	-0.044194000
1	-4.495315000	-2.246724000	1.375787000
1	-3.738655000	-3.559462000	3.326210000
1	-1.319738000	-3.741266000	3.860371000
1	1.321416000	-3.741469000	3.857137000
1	3.739005000	-3.560067000	3.316869000
1	4.491005000	-2.247385000	1.364618000
1	2.849770000	-1.046818000	-0.051266000
1	-2.857481000	1.046483000	-0.044194000
1	-4.495315000	2.246723000	1.375788000
1	-3.738654000	3.559462000	3.326211000
1	-1.319738000	3.741266000	3.860371000
1	1.321417000	3.741469000	3.857138000
1	3.739006000	3.560066000	3.316868000
1	4.491005000	2.247385000	1.364618000
1	2.849770000	1.046818000	-0.051266000
1	-0.001445000	-2.884669000	-1.409782000
1	0.002205000	-4.518239000	-3.278984000
1	0.006663000	-3.742669000	-5.623436000
1	0.007550000	-1.317775000	-6.152584000

1	0.007550000	1.317776000	-6.152584000
1	0.006663000	3.742669000	-5.623436000
1	0.002205000	4.518239000	-3.278984000
1	-0.001446000	2.884669000	-1.409782000

Raman frequencies (in cm^{-1}) and activities of 1 (B3LYP-D3/6-311+G optimized). Only frequencies, whose activities are larger than 10, are shown.**

Frequency	Activity	Frequency	Activity	Frequency	Activity
3.8164	19.257	1134.3	16.386	1614.2	59.879
26.306	13.453	1139.5	140.83	1616.2	18.347
30.19	52.636	1151.3	11.675	1633.1	737.18
97.166	403.29	1184.7	212.98	1634.6	84.825
138.54	42.126	1186.3	27.187	1636.9	574.93
165.25	326.05	1190.5	57.864	1640.8	138.72
216.73	11.631	1198.3	104.25	1641.6	397.59
296.41	34.117	1219.5	28.48	1645.3	178.21
331.63	701.76	1223	535.08	1776.8	1801.3
420.26	25.716	1230.2	411.96	3160.1	45.04
523.22	10.745	1232.7	43.394	3160.2	99.559
567.3	289.71	1234.1	114.44	3160.2	98.799
624.32	95.79	1242.5	107.45	3171.1	22.485
707.61	26.562	1317.9	247.46	3172	147.34
748.55	10.55	1319.7	15.429	3172.7	338.98
751.41	11.414	1321.5	87.213	3172.9	273.13
752.55	47.352	1330.9	38.5	3182.8	104.85
770.67	24.177	1350	770.85	3183.3	220.31
773.89	66.933	1367.8	18.204	3184.5	219.64
823.07	153.97	1385.7	77.73	3184.9	206.37
912.99	24.767	1388.1	40.189	3185.5	89.872
1018.3	109.24	1390.9	363.27	3186.1	1002.4
1021.9	23.397	1466.3	38.329	3193.2	18.969
1024	12.762	1466.3	285.55	3193.5	444.3
1039.6	14.088	1477.1	169.96	3202.1	20.526
1041.8	286.57	1496.8	60.983	3217.1	19.788
1045.7	23.585	1501.4	66.769	3217.4	160.5
1054.4	28.67	1502.8	72.003		
1116.2	60.035	1508.2	550.79		
1121.4	230.81	1609.3	11.491		

Total energies of the singlet and triplet states of 1 at 90, 100, 200, and 300 K, estimated by the B3LYP-D3/6-311+G calculation.**

Temperature(K)	$E_{singlet}$(hartree)	$E_{triplet}$(hartree)
90	-1539.1294751	-1539.0768378
100	-1538.7717156	-1538.7165715
200	-1538.7696856	-1538.7068850
300	-1538.6293748	-1538.5640721

Density matrix of the CASSCF(6,6)/6-311G* calculation for 1 at 90, 100, 200, and 300 K.

1 at 90 K

	1	2	3	4	5
1	0.199986D+01				
2	0.263613D-03	0.199982D+01			
3	-0.283250D-06	0.324044D-06	0.187249D+01		
4	-0.598795D-05	0.806092D-05	0.181842D-05	0.127528D+00	
5	-0.295697D-04	0.438654D-04	0.106904D-05	0.132194D-05	0.297083D-03
6	-0.799180D-05	0.514021D-05	0.782966D-05	-0.407525D-07	0.238953D-04

	6
6	0.170740D-05

1 at 100 K

	1	2	3	4	5
1	0.195579D+01				
2	0.831392D-05	0.199997D+01			
3	0.199665D-04	-0.800633D-06	0.187529D+01		
4	-0.247189D-03	0.641701D-04	0.101852D-03	0.125723D+00	
5	0.464592D-04	-0.418088D-04	0.137612D-03	0.216685D-07	0.138816D-04
6	0.460518D-04	0.527805D-04	0.178357D-03	0.234627D-05	-0.272185D-05

	6
6	0.432085D-01

1 at 200 K

	1	2	3	4	5
1	0.195719D+01				
2	0.593107D-05	0.199998D+01			
3	0.118206D-04	-0.898684D-06	0.189044D+01		
4	-0.289650D-04	0.186170D-05	0.323647D-05	0.110467D+00	
5	0.240561D-05	-0.607816D-06	0.368774D-05	-0.542667D-06	0.934101D-05
6	0.348638D-04	0.181422D-05	-0.120558D-04	0.900081D-05	-0.254146D-05

	6
6	0.419110D-01

1 at 300 K

	1	2	3	4	5
1	0.195812D+01				
2	0.997230D-05	0.199997D+01			
3	0.129305D-04	-0.269575D-05	0.189428D+01		
4	-0.740164D-04	-0.777337D-06	0.309219D-04	0.106583D+00	
5	0.105289D-04	0.169538D-05	0.386113D-04	-0.384942D-06	0.878242D-05
6	0.409905D-04	0.308203D-04	0.500721D-04	0.688924D-05	-0.218815D-05

	6
6	0.410348D-01

X-ray crystallographic data

Crystallographic data and structure refinement for **1** (90 K)

Data deposition	CCDC 1995679
Empirical formula	$C_{40}H_{24}$
Formula weight	504.49
Temperature	90 K
Wavelength	0.71073
Crystal system	monoclinic
Space group	$P2_1/c$
Unit cell dimensions	a = 9.4181(1) Å b = 9.0870(1) Å β = 98.5995(8)° c = 30.2502(4) Å
Volume	2559.78(5) Å^3
Z	4
Density (calculated)	1.309 Mg/m^3
Absorption coefficient	0.074 mm^{-1}
F(000)	1056.0
Crystal size	0.14 x 0.10 x 0.05 mm^3
Theta range for data collection	1.362 to 52.038°
Index ranges	–20<=h<=20, –20<=k<=19, –67<=l<=67
Reflections collected	151624
Independent reflections	19007
Completeness	0.986
Absorption correction	multi-scan
Refinement method	Full-matrix least-squares on F^2
Data / restraints / parameters	19007 / 0 / 1116
Goodness-of-fit on F^2	1.0852
Final R indices [I > 3sigma(I)]	$R1$ = 0.0284, w$R2$ = 0.0517
Largest diff. peak and hole	0.281 and –0.256 e • Å^{-3}

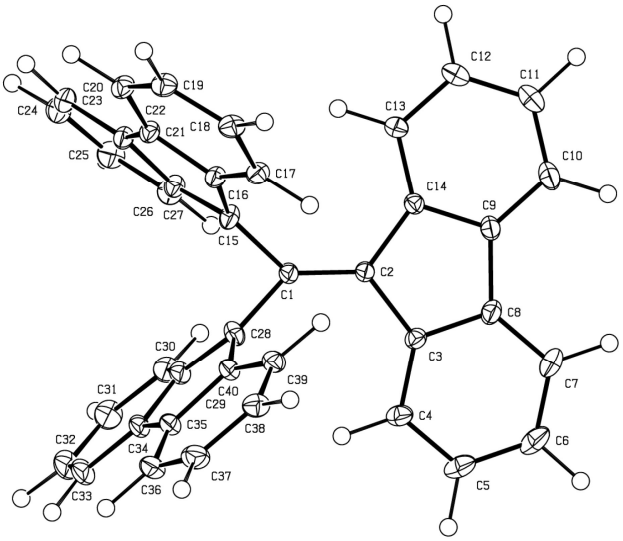

ORTEP drawing of **1** (at 90K). Thermal ellipsoids are drawn at the 50% probability level.

Crystallographic data and structure refinement for **1** (100 K)

Data deposition	CCDC 2062007
Empirical formula	$C_{40}H_{24}$
Formula weight	504.49
Temperature	100 K
Wavelength	0.71073
Crystal system	monoclinic
Space group	$P2_1/c$
Unit cell dimensions	a = 9.41782(16) Å b = 908189(14) Å β = 98.6279(15)° c = 30.2784(4) Å
Volume	2560.45(7) Å^3
Z	4
Density (calculated)	1.309 Mg/m^3
Absorption coefficient	0.074 mm^{-1}
F(000)	1056.0
Crystal size	0.139 x 0.116 x 0.103 mm^3
Theta range for data collection	2.343 to 27.498°
Index ranges	–12<=h<=12, –11<=k<=11, –39<=l<=39
Reflections collected	55025
Independent reflections	5864
Completeness	0.999
Absorption correction	multi-scan
Refinement method	Full-matrix least-squares on F^2
Data / restraints / parameters	5864 / 0 / 361
Goodness-of-fit on F^2	1.046
Final R indices [I > 2sigma(I)]	R1 = 0.0415, wR2 = 0.090
Largest diff. peak and hole	0.308 and –0.187 e • Å^{-3}

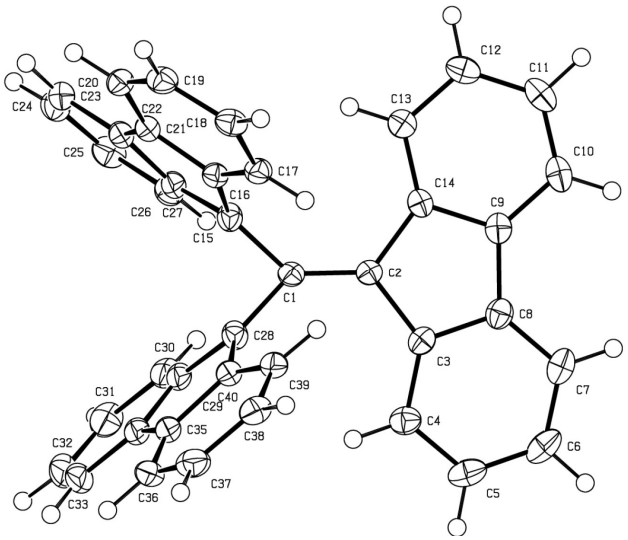

ORTEP drawing of **1** (at 100K). Thermal ellipsoids are drawn at the 50% probability level.

Crystallographic data and structure refinement for **1** (150 K)

Data deposition	CCDC 2062017
Empirical formula	$C_{40}H_{24}$
Formula weight	504.49
Temperature	150 K
Wavelength	0.71073
Crystal system	monoclinic
Space group	$P2_1/c$
Unit cell dimensions	a = 9.322(2) Å b = 9.08269(18) Å β = 98.741(2)° c = 30.4391(6) Å
Volume	2577.42(9) Å^3
Z	4
Density (calculated)	1.300 Mg/m^3
Absorption coefficient	0.074 mm^{-1}
F(000)	1056.0
Crystal size	0.139 x 0.116 x 0.103 mm^3
Theta range for data collection	2.342 to 27.499°
Index ranges	–12<=h<=12, –11<=k<=11, –39<=l<=39
Reflections collected	55346
Independent reflections	5905
Completeness	0.998
Absorption correction	multi-scan
Refinement method	Full-matrix least-squares on F^2
Data / restraints / parameters	5905 / 0 / 361
Goodness-of-fit on F^2	1.042
Final R indices [I > 2sigma(I)]	R1 = 0.0413, wR2 = 0.0998
Largest diff. peak and hole	0.263 and –0.169 e • Å^{-3}

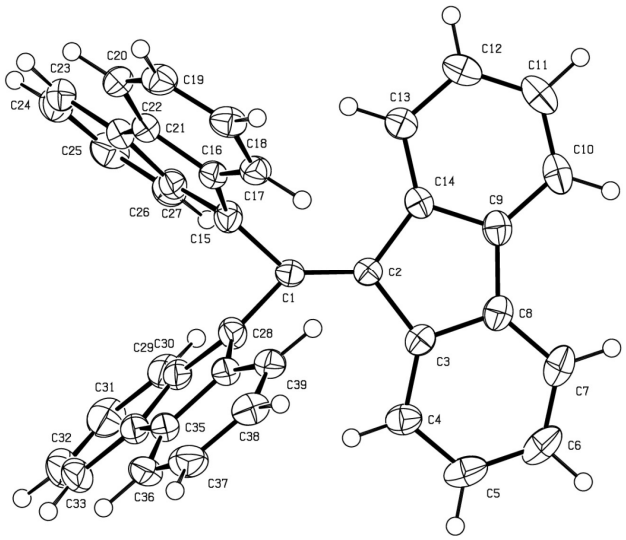

ORTEP drawing of **1** (at 150K). Thermal ellipsoids are drawn at the 50% probability level.

Crystallographic data and structure refinement for **1** (200 K)

Data deposition	CCDC 1995680
Empirical formula	$C_{40}H_{24}$
Formula weight	504.49
Temperature	200 K
Wavelength	0.71073
Crystal system	monoclinic
Space group	$P2_1/c$
Unit cell dimensions	a = 9.45015(19) Å b = 9.08872(17) Å β = 98.8206(18)° c = 30.5831(6) Å
Volume	2595.71(9) Å^3
Z	4
Density (calculated)	1.291 Mg/m^3
Absorption coefficient	0.073 mm^{-1}
F(000)	1056.0
Crystal size	0.139 x 0.116 x 0.103 mm^3
Theta range for data collection	2.340 to 27.498°
Index ranges	–12<=h<=12, –11<=k<=11, –39<=l<=39
Reflections collected	55756
Independent reflections	5941
Completeness	0.999
Absorption correction	multi-scan
Refinement method	Full-matrix least-squares on F^2
Data / restraints / parameters	5941 / 0 / 361
Goodness-of-fit on F^2	1.027
Final R indices [I > 2sigma(I)]	R1 = 0.0423, wR2 = 0.1021
Largest diff. peak and hole	0.230 and –0.144 e • Å^{-3}

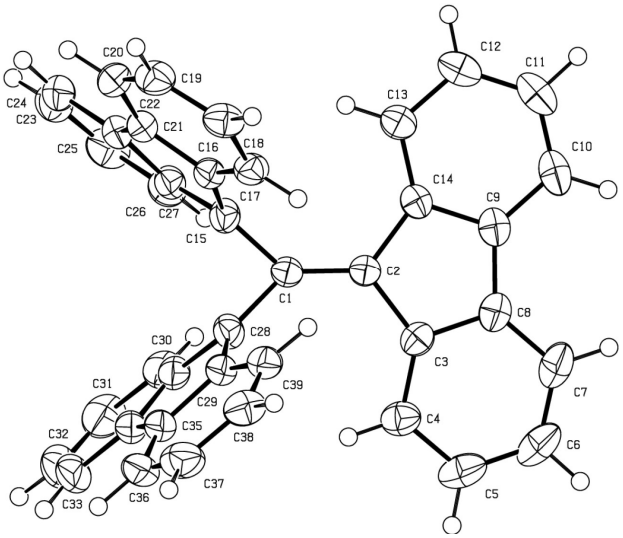

ORTEP drawing of **1** (at 200K). Thermal ellipsoids are drawn at the 50% probability level.

Crystallographic data and structure refinement for **1** (250 K)

Data deposition	CCDC 2062018
Empirical formula	$C_{40}H_{24}$
Formula weight	504.49
Temperature	250 K
Wavelength	0.71073
Crystal system	monoclinic
Space group	$P2_1/c$
Unit cell dimensions	a = 9.4559(2) Å b = 9.0809(2) Å β = 98.879(2)° c = 30.6814(7) Å
Volume	2602.98(10) Å^3
Z	4
Density (calculated)	1.288 Mg/m^3
Absorption coefficient	0.073 mm^{-1}
F(000)	1056.0
Crystal size	0.139 x 0.116 x 0.103 mm^3
Theta range for data collection	2.341 to 27.498°
Index ranges	–12<=h<=12, –11<=k<=11, –39<=l<=39
Reflections collected	56112
Independent reflections	5965
Completeness	0.999
Absorption correction	multi-scan
Refinement method	Full-matrix least-squares on F^2
Data / restraints / parameters	5965 / 0 / 361
Goodness-of-fit on F^2	1.024
Final R indices [I > 2sigma(I)]	R1 = 0.0435, wR2 = 0.1101
Largest diff. peak and hole	0.211 and –0.154 e • Å^{-3}

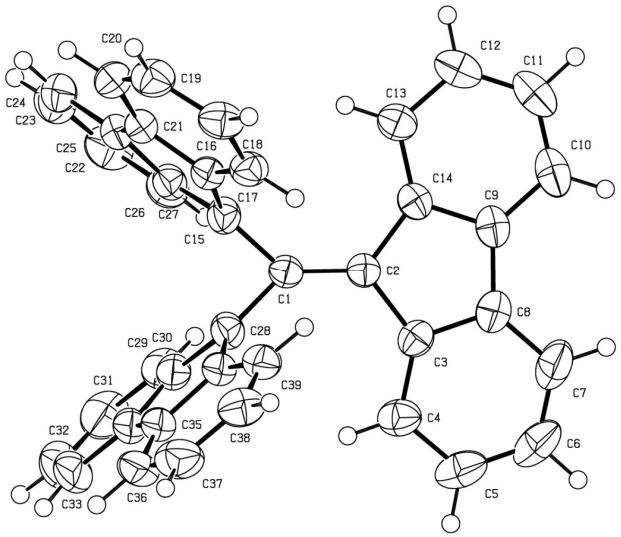

ORTEP drawing of **1** (at 250K). Thermal ellipsoids are drawn at the 50% probability level.

Crystallographic data and structure refinement for **1** (300 K)

Data deposition	CCDC 2062019
Empirical formula	$C_{40}H_{24}$
Formula weight	504.49
Temperature	300 K
Wavelength	0.71073
Crystal system	monoclinic
Space group	$P2_1/c$
Unit cell dimensions	a = 9.4698(2) Å b = 9.0813(2) Å β = 98.937(2)° c = 30.8006(8) Å
Volume	2616.64(11) Å^3
Z	4
Density (calculated)	1.282 Mg/m^3
Absorption coefficient	0.073 mm^{-1}
F(000)	1056.0
Crystal size	0.139 x 0.116 x 0.103 mm^3
Theta range for data collection	2.340 to 27.499°
Index ranges	–12<=h<=12, –11<=k<=11, –40<=l<=40
Reflections collected	56343
Independent reflections	6000
Completeness	0.999
Absorption correction	multi-scan
Refinement method	Full-matrix least-squares on F^2
Data / restraints / parameters	6000 / 0 / 361
Goodness-of-fit on F^2	1.035
Final R indices [I > 2sigma(I)]	R1 = 0.0456, wR2 = 0.1151
Largest diff. peak and hole	0.169 and –0.147 e • Å^{-3}

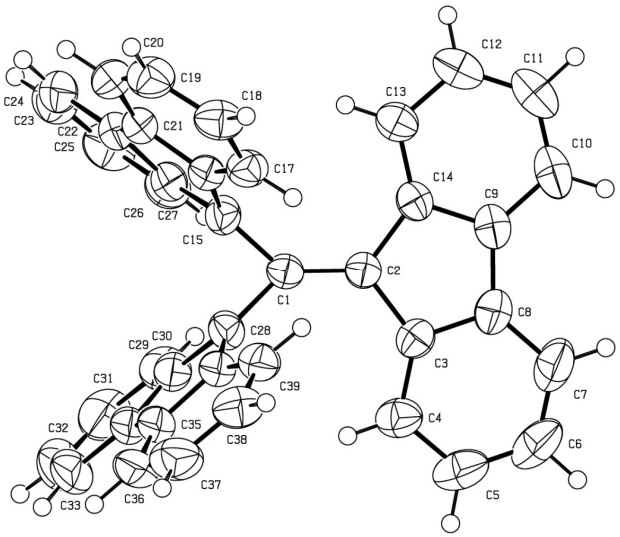

ORTEP drawing of **1** (at 300K). Thermal ellipsoids are drawn at the 50% probability level.

Crystallographic data and structure refinement for **1** (350 K)

Data deposition	CCDC 2062024
Empirical formula	$C_{40}H_{24}$
Formula weight	504.49
Temperature	350 K
Wavelength	0.71073
Crystal system	monoclinic
Space group	$P2_1/c$
Unit cell dimensions	a = 9.5008(2) Å b = 9.0966(2) Å β = 99.013(2)° c = 30.9861(8) Å
Volume	2644.91(11) Å^3
Z	4
Density (calculated)	1.267 Mg/m^3
Absorption coefficient	0.073 mm^{-1}
F(000)	1056.0
Crystal size	0.139 x 0.116 x 0.103 mm^3
Theta range for data collection	2.336 to 27.498°
Index ranges	–12<=h<=12, –11<=k<=11, –40<=l<=40
Reflections collected	57041
Independent reflections	6071
Completeness	0.999
Absorption correction	multi-scan
Refinement method	Full-matrix least-squares on F^2
Data / restraints / parameters	6071 / 0 / 361
Goodness-of-fit on F^2	1.036
Final R indices [I > 2sigma(I)]	R1 = 0.0476, wR2 = 0.1194
Largest diff. peak and hole	0.157 and –0.156 e • Å^{-3}

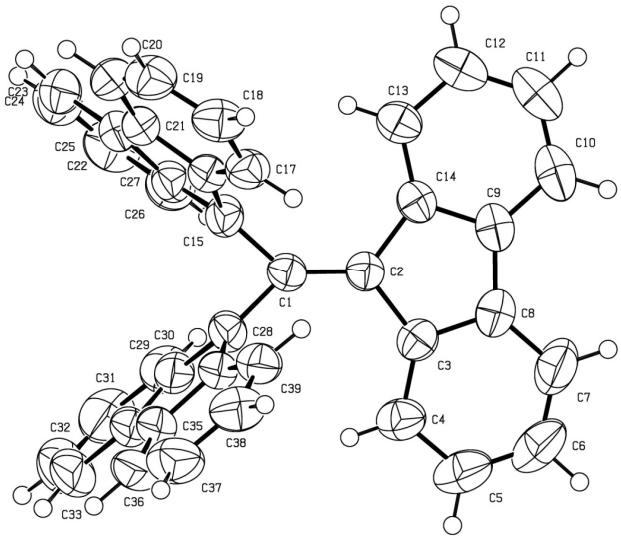

ORTEP drawing of **1** (at 350K). Thermal ellipsoids are drawn at the 50% probability level.

Crystallographic data and structure refinement for **1** (400 K)

Data deposition	CCDC 2062025
Empirical formula	$C_{40}H_{24}$
Formula weight	504.49
Temperature	400 K
Wavelength	0.71073
Crystal system	monoclinic
Space group	$P2_1/n$
Unit cell dimensions	a = 9.5092(3) Å
	b = 9.0954(3) Å β = 99.036(3)°
	c = 31.0567(10) Å
Volume	2652.76(15) Å^3
Z	4
Density (calculated)	1.263 Mg/m^3
Absorption coefficient	0.072 mm^{-1}
F(000)	1056.0
Crystal size	0.139 x 0.116 x 0.103 mm^3
Theta range for data collection	2.336 to 27.499°
Index ranges	–12<=h<=12, –11<=k<=11, –40<=l<=40
Reflections collected	57128
Independent reflections	6089
Completeness	0.999
Absorption correction	multi-scan
Refinement method	Full-matrix least-squares on F^2
Data / restraints / parameters	6089 / 0 / 361
Goodness-of-fit on F^2	1.023
Final R indices [I > 2sigma(I)]	R1 = 0.0470, wR2 = 0.1244
Largest diff. peak and hole	0.153 and –0.144 e • Å^{-3}

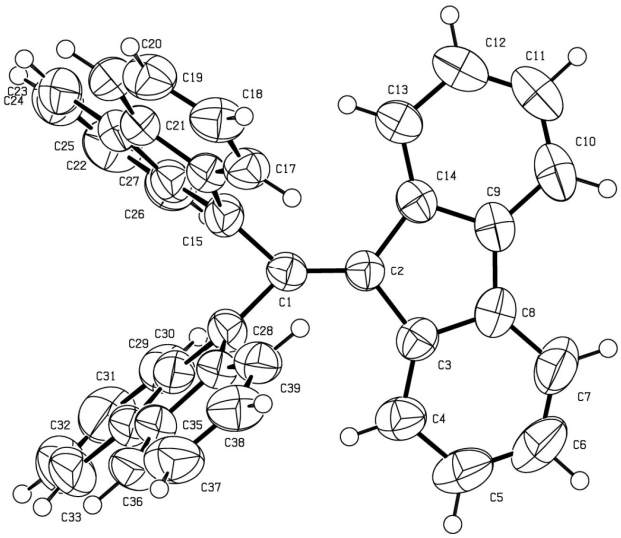

ORTEP drawing of **1** (at 400K). Thermal ellipsoids are drawn at the 50% probability level.

Crystallographic data and structure refinement for **2a**

Data deposition	CCDC 1995683
Empirical formula	C_{40} H_{26}
Formula weight	506.61
Temperature	150 K
Wavelength	0.71075
Crystal system	monoclinic
Space group	$P2_1/n$
Unit cell dimensions	a = 16.4306(6) Å
	b = 7.5182(2) Å β = 103.395(7)°
	c = 21.6031(7) Å
Volume	2596.01(16) Å^3
Z	4
Density (calculated)	1.296 Mg/m^3
Absorption coefficient	0.073 mm^{-1}
F(000)	1064.0
Crystal size	0.25 x 0.10 x 0.05 mm^3
Theta range for data collection	1.938 to 27.461°
Index ranges	–21<=h<=21, –9<=k<=8, –28<=l<=27
Reflections collected	23989
Independent reflections	5928
Completeness	0.997
Absorption correction	none
Refinement method	Full-matrix least-squares on F^2
Data / restraints / parameters	4556 / 0 / 465
Goodness-of-fit on F^2	1.010
Final R indices [I > 2sigma(I)]	R1 = 0.0434, wR2 = 0.0930
Largest diff. peak and hole	0.266 and –0.204 e • Å^{-3}

A level alerts were found in the checkCIF file:
PLAT410_ALERT_2_A Short Intra H...H Contact H2..H26. 1.83 Ang. x,y,z = 1_555 Check
PLAT410_ALERT_2_A Short Intra H...H Contact H11..H27. 1.85 Ang. x,y,z = 1_555 Check
Authors response: The short intramolecular contacts, which were pointed out at 'Alart B level' were found between sterically crowded fluorenylidene and two fluorenyl groups bonded to the central carbon atom, C40. 'H2' and 'H11' are the hydrogen atoms at 1- and 8-positions (C2 and C11, respectively) of the fluorenylidene group, respectively, and 'H26' and 'H27' are those at 9-position of each of two fluorenyl groups (C26 and C27, respectively). The hydrogen atoms were located on the difference Fourier maps and refined their positions and isotropic temperature factors.

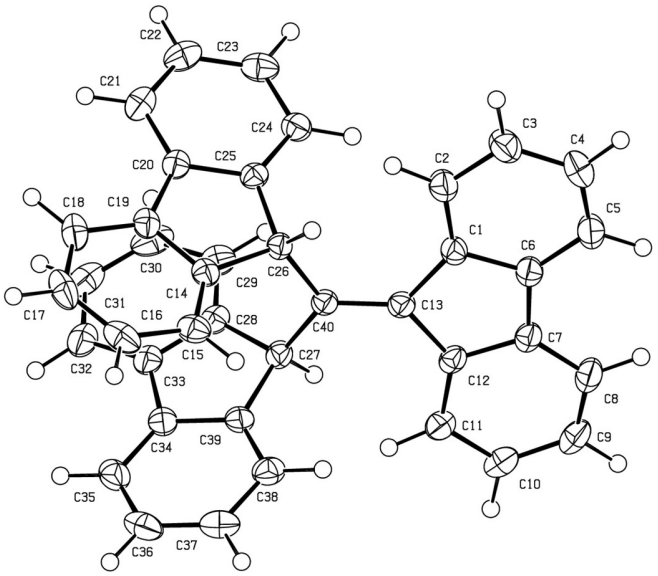

ORTEP drawing of **2a**. Thermal ellipsoids are drawn at the 50% probability level.

Crystallographic data and structure refinement for **3**

Data deposition	CCDC 1995682
Empirical formula	C_{72} H_{88} Li_2 O_8
Formula weight	1095.30
Temperature	200 K
Wavelength	0.71075
Crystal system	orthorhombic
Space group	$P2_12_12_1$
Unit cell dimensions	a = 17.2782(6) Å
	b = 17.5532(6) Å
	c = 41.2439(12) Å
Volume	12508.8(7) Å^3
Z	8
Density (calculated)	1.163 Mg/m^3
Absorption coefficient	0.073 mm^{-1}
F(000)	4720.0
Crystal size	0.20 x 0.20 x 0.10 mm^3
Theta range for data collection	2.220 to 27.486°
Index ranges	–22<=h<=22, –22<=k<=22, –53<=l<=53
Reflections collected	113973
Independent reflections	28667
Completeness	1.00
Absorption correction	none
Refinement method	Full-matrix least-squares on F^2
Data / restraints / parameters	11545 / 0 / 1477
Goodness-of-fit on F^2	0.933
Final R indices [I > 2sigma(I)]	R1 = 0.0742, wR2 = 0.1543
Largest diff. peak and hole	0.213 and –0.188 e • Å^{-3}

A level alerts were found in the checkCIF file:
PLAT241_ALERT_2_B High 'MainMol' Ueq as Compared to Neighbors of C102 Check
PLAT241_ALERT_2_B High 'MainMol' Ueq as Compared to Neighbors of C110 Check
PLAT242_ALERT_2_B Low 'MainMol' Ueq as Compared to Neighbors of C101 Check
PLAT340_ALERT_3_B Low Bond Precision on C-C Bonds ..... 0.01051 Ang.
Authors response: These alerts are a consequence of disorders in a solvent molecule (tetrahydrofuran) coordinated to a lithium ion.
PLAT910_ALERT_3_B Missing # of FCF Reflection(s) Below Theta(Min).
Authors response: The unit cell is reasonable large and these low angle reflections are probably missing due to the beam stop.

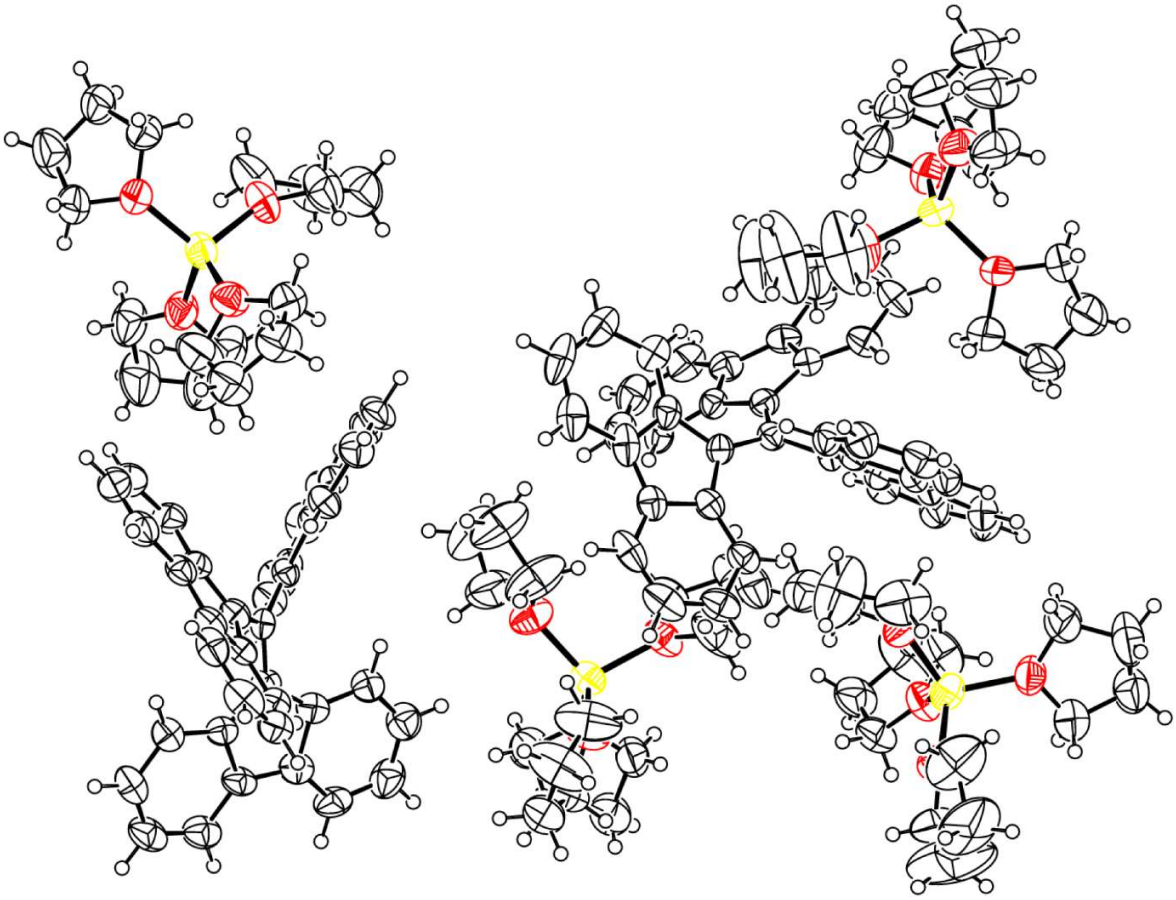

ORTEP drawing of **3**. Thermal ellipsoids are drawn at the 50% probability level.

Validation of structure of 1 at 90 K

The structure was minutely examined whether the structural modeling was sufficient or not by means of the Hirshfeld's rigid bond test[S9] and the Fourier analysis. In order to avoid the contribution of valence electrons on the structure, we used the structure derived from the high-order refinements for testing. As described in 'X-ray electron density distribution analysis of **1**' section, high order refinements were carried out using 24397 independent reflections with $\sin\theta/\lambda \geq 0.60$ Å^{-1}, which is enough to cut the contribution of valence electrons off from the diffraction data (Fig. S16). The C–H distance was constrained at 1.083 Å during the refinements.

On the Hirshfeld's rigid bond test, if $z^2_{A,B}$ denotes the mean square displacement amplitude of atom A in the direction of atom B, then for every covalently bonded pair of atoms A and B, the difference of mean-squares displacement amplitude, DMSDA ($\Delta_{A,B}$) should be zero, i.e.

$$\Delta_{A,B} = z^2_{A,B} - z^2_{B,A} = 0.$$

According to Hirshfeld, the difference of mean-squares displacement amplitude, DMSDA ($\Delta_{A,B}$), should normally be smaller than 0.001 Å^2 if atoms are at least as heavy as carbon. Conversely, if the DMSDA is significantly large, one may deduce that the structural model is insufficient, and a disordered model should be introduced. In the case of **1**, the DMSDAs were calculated to be ≤ 0.001 Å^2 for every atomic pair forming chemical bond. The small DMSDAs suggest the structure of **1** was sufficiently described as an ordered structure. Furthermore, the Fourier analysis based on the difference Fourier maps also showed that no remarkable residual density observed at ± 0.1 e Å^{-3} level, where $\Delta\rho_{\min,\max} = -0.230, 0.275$ e Å^{-3} (Fig. S17). These results clearly indicate that the molecule of **1** adopts the ordered structure in the crystalline state.

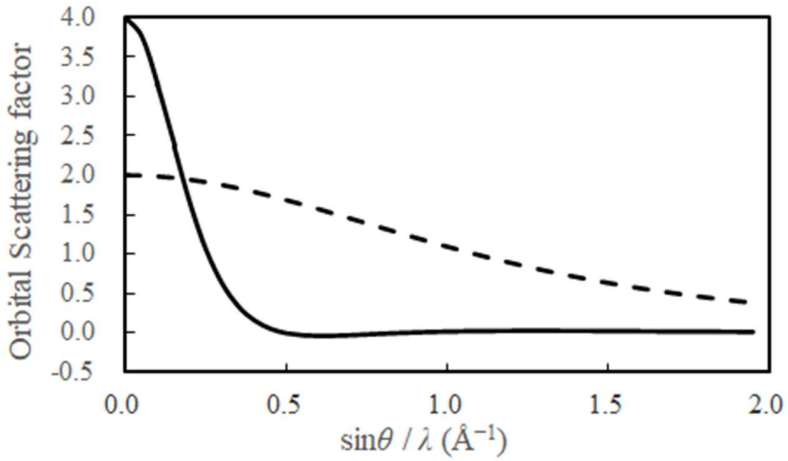

Fig. S16.
Orbital scattering factors for carbon atom. Solid and dashed lines indicate contribution of valence and core electrons, respectively. The contribution of valence electrons vanishes above 0.5 Å^{-1} in $\sin\theta/\lambda$ [S10].

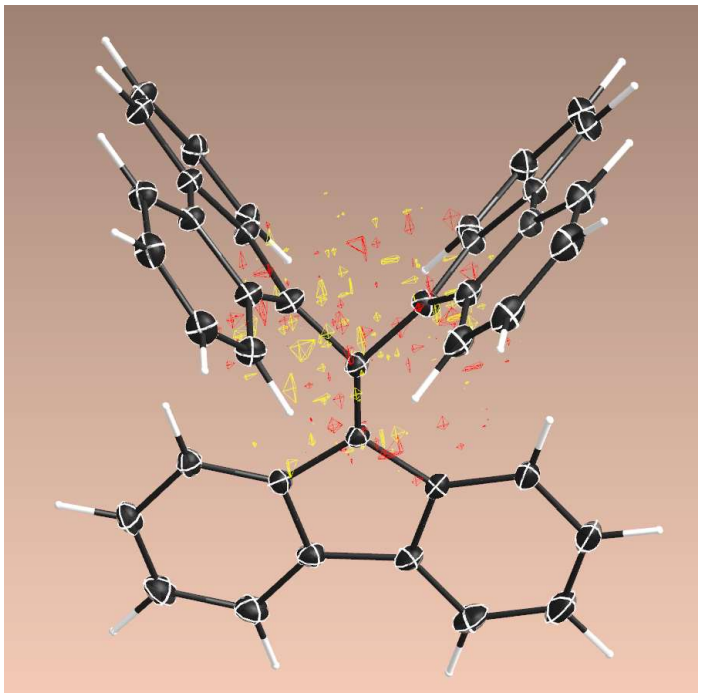

Fig. S17.
3D-isosurface difference Fourier map of **1** at 90 K at ± 0.1 e Å^{-3}. Yellow and red surfaces indicate positive and negative electron density distribution, respectively.

References

S1. Gaussian 16, Revision B.01. Frisch, M. J.; Trucks, G. W.; Schlegel, H. B.; Scuseria, G. E.; Robb, M. A.; Cheeseman, J. R.; Scalmani, G.; Barone, V.; Petersson, G. A.; Nakatsuji, H.; Li, X.; Caricato, M.; Marenich, A. V.; Bloino, J.; Janesko, B. G.; Gomperts, R.; Mennucci, B.; Hratchian, H. P.; Ortiz, J. V.; Izmaylov, A. F.; Sonnenberg, J. L.; Williams-Young, D.; Ding, F.; Lipparini, F.; Egidi, F.; Goings, J.; Peng, B.; Petrone, A.; Henderson, T.; Ranasinghe, D.; Zakrzewski, V. G.; Gao, J.; Rega, N.; Zheng, G.; Liang, W.; Hada, M.; Ehara, M.; Toyota, K.; Fukuda, R.; Hasegawa, J.; Ishida, M.; Nakajima, T.; Honda, Y.; Kitao, O.; Nakai, H.; Vreven, T.; Throssell, K.; Montgomery, J. A., Jr.; Peralta, J. E.; Ogliaro, F.; Bearpark, M. J.; Heyd, J. J.; Brothers, E. N.; Kudin, K. N.; Staroverov, V. N.; Keith, T. A.; Kobayashi, R.; Normand, J.; Raghavachari, K.; Rendell, A. P.; Burant, J. C.; Iyengar, S. S.; Tomasi, J.; Cossi, M.; Millam, J. M.; Klene, M.; Adamo, C.; Cammi, R.; Ochterski, J. W.; Martin, R. L.; Morokuma, K.; Farkas, O.; Foresman, J. B.; Fox, D. J. Gaussian, Inc., Wallingford CT (2016).

S2. Lu, T.; Chen, F. Multiwfn: A multifunctional wavefunction analyzer. *J. Comput. Chem.* **33**, 580–592 (2012).

S3. HKL2000, Otwinoski, Z.; Minor, W. *Methods in Enzymol*. **276**, 307–326 (1997).

S4. SHELXT, Sheldrick, G. M. *Acta Crystallogr. Sect. A* **71**, 3–8 (2015).

S5. Hansen, N. K.; Coppens, P. *Acta Crystallogr. Sect. A* **34**, 909–921 (1978).

S6. XD2006 – a computer program for multipole refinement, topological analysis of charge densities and evaluation of intermolecular energies from experimental or theoretical structure factors. Volkov, A.; Macchi, P.; Farrugia, L. J.; Gatti, C.; Mallinson, P. R.; Richter, T.; Koritsanszky, T. (2006).

S7. Lodewyk, M. W.; Siebert, M. R.; Tantillo, D. J. *Chem. Rev.* **112**, 1839–1862 (2012).

S8. Winkler, M.; Sander, W. *J. Phys. Chem. A* **105**, 10422–10432 (2001).

S9. Hirshfeld, F. L. *Acta Crystallogr. Sect. A*, **A32**, 239–244 (1976).

S10. Macchi, P.; Coppens, P. *Acta Crystallogr. Sect. A*, **A57**, 656–662 (2001).